BELLCOMM, INC.
1100 SEVENTEENTH STREET, N.W.   WASHINGTON, D.C.   20036

COVER SHEET FOR TECHNICAL MEMORANDUM

TITLE- Error Analysis of Orbit Determination
for Mars Orbiters

TM-69-1014-1

DATE- January 23, 1969

FILING CASE NO(S)- 105-3

AUTHOR(S)- S. S. Bayliss

FILING SUBJECT(S)-   Orbit Determination
(ASSIGNED BY AUTHOR(S)-

ABSTRACT

The orbital parameters of a planetary artificial
satellite can be estimated using range-rate measurements taken
from earth. Results of a computer simulation show that the error
bounds given by the covariance matrix provide a conservative
upper limit for errors in the estimated parameters.

The accuracy of the estimated parameters is a function
of both data point spacing and total tracking time. Good results
are obtained for tracking times of 30-40 hours. Including the
estimation of the gravitational parameter decreases the accuracy
of the estimation of the orbital parameters significantly.

SEE REVERSE SIDE FOR DISTRIBUTION LIST

SUBJECT: Error Analysis of Orbit
Determination for Mars
Orbiters - Case 105-3

DATE: January 23, 1969

FROM: S. S. Bayliss
TM-69-1014-1

TECHNICAL MEMORANDUM

I. Introduction

        This paper presents a continuation of the work
described in Reference 2. That report presented several
techniques for estimating the orbital parameters of planetary
artificial satellites and the planetary gravitational parameter.
This work presents a more detailed analysis of the accuracy
to which the method of differential correction with a least
squares estimation criterion can be expected to converge. The
analysis is performed for a simplified case of a satellite
orbiting Mars and being tracked from earth. The Doppler
measurements for a set of orbital parameters are computed
and then corrupted by additive random noise with a normal
distribution. The method of differential corrections is then
used to estimate the orbital parameters of the satellite from
these noisy measurements. The covariance matrix for the errors
in the estimation is generated for the nominal orbital para-
meters of the satellite and is a bound on these errors. The
method presented here is self-contained but is primarily intended
to supplement Reference 2. Therefore, some material which has
been treated fairly completely in that paper has been covered
rather superficially here.

II. Physical Model

    A) Coordinate Systems: For this study, we will use three
coordinate systems. These are:

        1) Sun-Centered Ecliptic. The origin of the coordinate
            system is located at the center of the sun and the
            z-axis is perpendicular to the plane of the ecliptic
            pointing toward celestial north. The positive x-axis
            is in the ecliptic and points to the vernal equinox
            of the earth. The y-axis is in the ecliptic and com-
            pletes the right hand coordinate system.

        2) Planet-Centered Ecliptic. Identical in orientation
            to the sun-centered ecliptic frame but with its origin
            at the center of the planet.

3) Planet-Centered Satellite Plane. The origin of the coordinate system is at the center of the planet and the positive z-axis is perpendicular to the satellite plane and parallel to the satellite angular momentum vector. The x-axis is in the satellite orbital plane and points through the satellite periapsis. The y-axis completes the right-hand set.

The position and velocity of a satellite in a Keplerian orbit may be completely specified by time and the six orbital constants

a = semi-major axis

e = eccentricity

τ = time of periapsis passage

i = inclination

ω = **argument** of periapsis

Ω = longitude of ascending node.

The variables a and e define the size and shape of the orbit, τ allows us to relate true anomaly to absolute time, and $i, \omega,$ and Ω are a set of Euler angles defining the orientation of the satellite orbital plane with respect to a reference frame. We also define

f = true anomaly

μ = gravitation parameter of the attracting mass.

The angular variables (i, ω, Ω, f) are illustrated in Figure 1.

In the satellite orbit plane, the magnitude of the radius vector is given by

$$r = \frac{a(1-e^2)}{1+e \cos f}. \tag{1}$$

The in-plane velocity components are given by

$$\dot{r} = \left[\frac{\mu}{a(1-e^2)} \right]^{1/2} e \sin f \tag{2}$$

$$\dot{rf} = \left[\frac{\mu}{a(1-e^2)} \right]^{1/2} (1+e \cos f). \qquad (3)$$

The relation between f and time is given by Kepler's equation

$$E - e \sin E = \sqrt{\frac{\mu}{a^3}} \ (t-\tau) \qquad (4)$$

where E = eccentric anomaly

and

$$\sin f = \frac{\sqrt{1-e^2} \ \sin E}{1-e \cos E}$$

$$\cos f = \frac{\cos E - e}{1-e \cos E} \ .$$

The coordinates in the planet-centered satellite plane are

$$x_3 = r \cos f; \qquad \dot{x}_3 = \dot{r} \cos f - \dot{rf} \sin f$$

$$y_3 = r \sin f; \qquad \dot{y}_3 = \dot{r} \sin f + \dot{rf} \cos f \qquad (5)$$

$$z_3 = 0; \qquad \dot{z}_3 = 0 \ .$$

To transform to the planet-centered ecliptic plane we require three successive coordinate rotations of $-\omega$, $-i$, and $-\Omega$ about the instantaneous z, x, and z axes, respectively. In vector-matrix notation, we have

$$\begin{bmatrix} x_2 \\ y_2 \\ z_2 \end{bmatrix} = \begin{bmatrix} \cos \Omega & -\sin \Omega & 0 \\ \sin \Omega & \cos \Omega & 0 \\ 0 & 0 & 1 \end{bmatrix} \begin{bmatrix} 1 & 0 & 0 \\ 0 & \cos i & -\sin i \\ 0 & \sin i & \cos i \end{bmatrix} \begin{bmatrix} \cos \omega & -\sin \omega & 0 \\ \sin \omega & \cos \omega & 0 \\ 0 & 0 & 1 \end{bmatrix} \begin{bmatrix} x_3 \\ y_3 \\ z_3 \end{bmatrix}$$

or

$$\underline{r}_2 = A\underline{r}_3 \quad . \tag{6}$$

Similarly, the velocity vector is transformed using

$$\underline{v}_2 = A\underline{v}_3 \quad . \tag{7}$$

It should be emphasized that the satellite orbital elements are referred to the planet-centered ecliptic reference frame and not the more common planet-centered equatorial frame. If it is desirable to refer the orbital elements to the equatorial frame (e.g., when perturbations due to higher order terms in the planetary gravitation field are to be included) Equations (6) and (7) must be written as

$$\underline{r}_2 = BA \ \underline{r}_3$$

$$\underline{v}_2 = BA \ \underline{v}_3 \tag{8}$$

where

$$B = \begin{bmatrix} \cos \alpha & -\sin \alpha & 0 \\ \sin \alpha & \cos \alpha & 0 \\ 0 & 0 & 1 \end{bmatrix} \begin{bmatrix} 1 & 0 & 0 \\ 0 & \cos i_o & -\sin i_o \\ 0 & \sin i_o & \cos i_o \end{bmatrix}$$

$$\begin{bmatrix} \cos \beta & -\sin \beta & 0 \\ \sin \beta & \cos \beta & 0 \\ 0 & 0 & 1 \end{bmatrix} \begin{bmatrix} 1 & 0 & 0 \\ 0 & \cos i_p & -\sin i_p \\ 0 & \sin i_p & \cos i_p \end{bmatrix}$$

and

α = angle between the vernal equinox of the earth and the ascending node of the orbit of Mars measured in the ecliptic plane

i_o = inclination of the Martian orbit

β = angle between the Martian ascending node and the Martian vernal equinox measured in the Martian orbital plane

i_p = inclination of the Martian polar axis to the Martian orbital plane.

B) Tracking Geometry

For simplicity, the earth is assumed to be in a circular orbit with its polar axis at zero inclination. Mars is assumed to be in an elliptical, inclined orbit with its polar axis inclined to its orbital plane. A satellite in an elliptical orbit about Mars is tracked by an antenna located on the surface of the earth. The following vectors are defined:

$\underline{R}(t)$ - location of the tracking antenna in an earth-centered ecliptic frame.

$\underline{D}(t)$ - vector from the center of Mars to the center of earth in a sun-centered ecliptic frame.

$\underline{r}(t)$ - location of the Mars satellite in a Mars-centered ecliptic frame.

The first two vectors are assumed known to a fairly high degree of accuracy. (This accuracy will be examined more closely in Appendix A). The third vector is what we wish to determine and is initially known only approximately. If we now define

$\underline{\rho}$ = vector from the tracking antenna to the satellite,

we see from Figure 2 that

$$\underline{\rho}(t) = \underline{r}(t) - \underline{D}(t) - \underline{R}(t)$$
$$\dot{\underline{\rho}}(t) = \dot{\underline{r}}(t) - \dot{\underline{D}}(t) - \dot{\underline{R}}(t) .$$

(9)

At the tracking station, we measure the Doppler shift of a signal sent from the station to the satellite and back again. This allows us to calculate* the relative velocity between the satellite and the antenna along the $\underline{\rho}$ direction. Thus, we can consider the measurements $F(t_i)$ taken by the tracking station to be

$$F(t_i) = \dot{\underline{\rho}}(t_i) \cdot \hat{\underline{\rho}}(t)$$

(10)

---

*Eq. (9) is approximate for the case of a real measurement program. See point (6) on page 15.

where $\hat{\rho}$ indicates a unit vector. The measured value of the Doppler shift is assumed to contain a random error. Our object is to use a sequence of N measurements taken at times t_1, t_2,..., t_N to determine the orbital parameters $(a,e,\tau,i,\omega,\Omega)$ of the satellite plus the gravitational parameter μ of Mars. The method we will use will be that of differential corrections.

III.   Method of Differential Corrections

A) Suppose we wish to estimate the m-component state vector, $\underline{x}$, of a system using a p-component measurement vector, $\underline{z}$, containing random errors, $\underline{v}$, which are independent of the state $\underline{x}$. If we assume the measurements to be linear functions of the state, we may write

$$\underline{z} = H\underline{x} + \underline{v} \tag{11}$$

where H is a known p by m matrix of constants. We also assume the measurement noise to be normally distributed with a zero mean, so that

$$E[\underline{v}] = \underline{0}$$

$$E[\underline{v}\,\underline{v}^T] = R \quad (\text{ a known p by p matrix}).$$

If the measurement process is nonlinear,

$$\underline{z}_i = F(\underline{x},t_i) + \underline{v} \tag{12a}$$

it is necessary to approximate the relation given in Equation (11). To do this, assume we have a first guess, $\overline{\underline{x}}$, for the state that is close to the actual solution, $\underline{x}$. Let the measurement vector corresponding to $\overline{\underline{x}}$ be given by $\overline{\underline{z}}$, i.e.,

$$\overline{\underline{z}}_i = F(\overline{\underline{x}},t_i) \quad .$$

Then, we may write

$$\underline{z}_i - \overline{\underline{z}}_i = F(\underline{x},t_i) - F(\overline{\underline{x}},t_i) + \underline{v}.$$

To first order, we may write

$$F(\underline{x},t_i) - F(\overline{\underline{x}},t_i) = \left[\frac{\partial F(\underline{x},t_i)}{\partial \underline{x}}\right]_{\underline{x} = \overline{\underline{x}}} (\underline{x} - \overline{\underline{x}})$$

If we let

$$\delta \underline{x} = \underline{x} - \overline{x}$$

$$\delta \underline{z} = \underline{z} - \overline{z} \quad,$$

then we have

$$\delta \underline{z}_i = \left[\frac{\partial F(\underline{x}, t_i)}{\partial \underline{x}} \right]_{\underline{x} = \overline{x}} \delta \underline{x} + \underline{v} \quad. \tag{12b}$$

If we set

$$H_{ij} = \left[\frac{\partial F(\underline{x}, t_i)}{\partial x_j} \right]_{\underline{x} = \overline{x}} \quad \begin{array}{l} (i = 1, \ldots, p) \\ (j = 1, \ldots, m), \end{array}$$

then we have the analogous form to Equation (11), where the value of the state, $\underline{x}$, has been replaced by its deviation, $\delta \underline{x}$.

Using a maximum likelihood estimator, we seek a weighted least-squares estimate, $\tilde{\underline{x}}$, that minimizes the cost function

$$J = \frac{1}{2} \left[(\delta \underline{x} - H \delta \underline{x})^T R^{-1} (\delta \underline{x} - H \delta \underline{x}) \right]. \tag{13}$$

In Reference (1) it is shown that the estimate is given by

$$\tilde{\underline{x}} = \overline{x} + PH^T R^{-1} (\delta \underline{z} - H \delta \underline{x}) \tag{14}$$

where

$$P^{-1} = H^T R^{-1} H. \tag{15}$$

We then set $\overline{x} = \underline{x}$ and repeat the iteration. It is also shown in Reference (1) that P is the covariance matrix for this estimate of the state, i.e.,

$$P = E[\underline{e} \, \underline{e}^T]$$

where

$$\underline{e} = \tilde{\underline{x}} - \underline{x} \quad.$$

Several techniques for implementing this algorithm (Equation 14) are given in Reference (2). In practice, it proved faster to use the nonlinear term

$$[\underline{z}_i - F(\underline{x}, t_i)]$$

to replace the linear approximation

$$[\delta\underline{z}_i - H\delta\underline{x}_i]$$

in the actual computation of Equation (14). Comparison of Equations (12a) and (12b) show that the two terms are equivalent.

B)   Application to the Problem

      For our problem, we define the state of the satellite by the six orbital elements

$$\underline{x}^T = [a, e, \tau, i, \omega, \Omega] \; .$$

When the gravitational parameter is being estimated, the state is enlarged to seven dimensions

$$\underline{x}^T = [a, e, \tau, i, \omega, \Omega, \mu] \; .$$

The measurement process

$$\underline{z}_i = F(\underline{x}, t_i)$$

is highly nonlinear and must be linearized as described in Equation (12b). The derivation of the partial derivatives for

$$H_{ij} = \frac{\partial F(\underline{x}, t_i)}{\partial x_j} \qquad j = 1, \ldots m \quad (m \text{ is either 6 or 7})$$

is given in Appendix B.

      The components of the measurement noise, v_i, are assumed to be uncorrelated, with a constant standard deviation. Thus

$$E[v_i v_j] = \sigma_i^2 \delta_{ij}$$

and therefore, the covariance matrix is the diagonal matrix

$$R = \sigma^2 I . \quad (I = p \text{ by } p \text{ identity matrix})$$

From Equations (14) and (15), we see that

$$\underline{x} = \overline{\underline{x}} + [H^T H]^{-1} H^T (\underline{z} - F(\overline{\underline{x}})) \tag{16}$$

$$P = \sigma^2 [H^T H]^{-1} . \tag{17}$$

The elements of the P matrix represent the expectations of the products of the errors in the components of $\underline{x}$, i.e.,

$$P_{ij} = E[\delta x_i \delta x_j] .$$

Thus, the diagonal elements of P represent the square of the standard deviation of each component of the state vector $\underline{x}$, while the off-diagonal elements represent the cross-correlation between errors in these elements.

If our first guess, $\overline{\underline{x}}$, is close enough to the solution point for the minimum of the cost function given in Equation (13), the iterative use of Equation (16) will lead us to that solution point. At this solution point, the covariance matrix, P, gives us some idea of the accuracy to which we have converged. An estimate of the best value of σ for the measurement noise for this particular problem is given in Appendix A.

IV. Simulation Results

For simulation purposes, Earth and Mars were assumed to move in Keplerian orbits with the following elements (defined with respect to the sun-centered ecliptic frame):

	Earth	Mars
a(km)	$1.495(10^8)$	$2.275(10^8)$
e	0.0	0.093368
τ(hrs)	0.0	0.0
i	0°	1.84991°
ω	0°	286.08176°
Ω	0°	49.24903°
μ(km^3/hrs^2)	$1.7199864(10^{18})$	$1.7199864(10^{18})$.

The tracking station was assumed to be located on the surface of the earth (R_E = 6378.16 km) at 35° N latitude, 117° W longitude. The angular velocity of the earth's rotation was taken as

$$\omega_{ie} = 7.2921158(10^{-5}) \text{ rad/sec.}$$

The earth's polar axis was assumed to have zero inclination. Using this information plus the nominal elements for the Mars orbiting satellite, the theoretical Doppler shift is calculated from Equations (9) and (10). For the cases simulated, the Doppler shifts calculated corresponded to relative velocities ranging from 27,500 km/hr (7600 m/sec) to 39,000 km/hr (10,800 m/sec). The main contribution to this was from $\underline{\dot{D}}(t)$, the relative velocity between earth and Mars. These measurements are then corrupted by additive random noise with a normal distribution having zero mean and a standard deviation of

$$\sigma = .152 \text{ km/hr} \quad (.0423 \text{ m/sec}) .$$

This set of corrupted measurements [$F(t_1)$, i = 1,2...,N] is then used to estimate the original orbital parameters.

From Equation (17), we may calculate the covariance matrix P using

$$P = \sigma^2 [H^T H]^{-1} .$$

Covariance matrices are evaluated at the nominal state values to avoid introducing effects caused by different solution points for different numbers of measurements and different sets of measurement noise.

The results of the computer simulation are illustrated in Figures 3 to 28. The values of the orbital parameters $(a,e,\tau,i,\omega,\Omega)$, the gravitational parameter (μ), and the data point spacing (Δt) used in simulating the measurements are given on each. Curves 1 and 2 in Figures 3 to 10 are the standard deviations for the estimates of the state variables as functions of tracking time for a rather elliptical (e = .574) orbit. Curves 3 and 4 in Figures 3 to 10 give the same quantities for a nearly circular (e = .05) orbit. Curves 1 and 3 are for a six dimension state vector and Curves 2 and 4 are for a seven dimension state. The predominant feature of these curves

is a rather sharp drop initially in the standard deviation
which changes into a more gradual decline as the tracking
time increases. The curves also appear to be modulated by
periodic terms whose predominant period is the orbital
period for curves 1 and 2 and half the orbital period for
curves 3 and 4. The first big drop in the standard devia-
tions levels off somewhat at the end of the first orbit of
tracking. Each succeeding orbit of tracking time adds a
diminishing amount to the accuracy of the esimate. It is
also interesting to note that each sharp drop in the standard
deviation curves for orbits with large eccentricity occurs
around periapsis. For those cases where

$$a = 12,760 \text{ km} ,$$

the satellite passes through periapsis at

$$t = 14.14 \text{ hrs}$$

$$26.28 \text{ hrs}$$

$$38.42 \text{ hrs}$$

$$50.56 \text{ hrs. }$$

The effect is most easily visible in Figure 3, curve 1. This
effect is due to the increased angular velocity of the satellite
near periapsis. Thus, the time rate of information on the shape
of the orbit is high near periapsis and low near apoapsis. For
orbits with low eccentricity (e.g., curves 3 and 4 on Figures 3
and 4, respectively), this effect is not present. Instead, a
term with about double the orbital frequency appears to modulate
the drop in the standard deviations.

Comparison of standard deviations between curves 1 and 2
and between curves 3 and 4 shows the effects of including the
estimation of the gravitational parameter. The standard devia-
tion of the semi-major axis (Figures 3 and 4) increases four
orders of magnitude when μ is estimated. Also, for the low
eccentricity case, the standard deviations of ω and Ω increase
by an order of magnitude (Figures 8 and 9, respectively). The
standard deviation of τ changes only slightly when μ is esti-
mated, but increases by an order of magnitude when we go from
a highly eccentric to a nearly circular orbit (Figure 6). The
standard deviation of μ also increases as eccentricity decreases
(Figure 10). The standard deviations of e and i appear to be
affected very little by changes in e or by including μ in the
estimation (Figures 5 and 7, respectively).

Figures 11-16 illustrate the effects of changing the data point spacing. Curves 1, 5, and 6 have a data point spacing of .5 hours, .1 hours and 1.0 hours, respectively. In general, an increase of the data point spacing from .5 hrs to 1.0 hrs (thereby halving the number of data points in a given time period) results in an increase of the standard deviations of about 45% to 60%. Decreasing the data point spacing to .1 hrs (using five times as many points in a given time period))yields a drop of only 50% to 60% in the standard deviations. The shapes of the curves of standard deviations vs. tracking time remain essentially the same and are merely shifted up or down.

Figures 17-22 show the effect of orbital period. The semi-major axis for curve 1 is 12,760 km and for curve 7 is 8960 km. The remaining orbital elements are identical for the two orbits.

Comparison of curves 1 and 7 shows that the accuracy for the estimates of a (Figure 17) and τ (Figure 19) are affected more by the number of orbits of tracking data (i.e., the angular length of orbit tracked) rather than the length of time the satellite is tracked. The orbit in curve 1 has a period of 12.1415 hrs while that in curve 7 has a period of 7.13 hrs. Periapsis for the 7.13 hr orbit occurs at

$$t = \quad 9.13 \text{ hrs}$$
$$16.26 \text{ hrs}$$
$$23.39 \text{ hrs}$$
$$30.52 \text{ hrs}$$
$$37.65 \text{ hrs}$$
$$44.78 \text{ hrs} .$$

and the drops in the standard deviations at these points are evident. The values for standard deviations of a and τ are consistently smaller for the shorter period orbit in curve 7, while those for e, i, ω and Ω are roughly the same for curves 1 and 7. Temporary large differences in them are due to the different orbital frequencies modulating their decrease. The increase in tracking accuracy of "a" results from the higher angular velocity associated with shorter period orbits. An error in "a" results in an error in period which causes a growing phase difference between the measured and calculated positions of the satellite. This shows up more rapidly for a shorter period satellite. For a similar reason, the accuracy of estimation of μ should increase faster for a short period

orbit. This effect can be seen in Equation (B7) in Appendix B, where the coefficients of the secular terms in $\frac{\partial F}{\partial a}$ and $\frac{\partial F}{\partial \mu}$ and the constant in $\frac{\partial F}{\partial \tau}$ vary inversely with a and hence inversely with the orbital period.

The standard deviations provide us with a useful bound on the magnitude of the errors since, for a normally distributed error,

$$\text{Prob } [\,|\delta x_i| \leq \sigma_{x_i}\,] = 68.27\%$$

$$\text{Prob } [\,|\delta x_i| \leq 2\sigma_{x_i}\,] = 95.45\%$$

$$\text{Prob } [\,|\delta x_i| \leq 3\sigma_{x_i}\,] = 99.73\%.$$

Figures 23-28 are a set of standard deviations and error values for a typical case. The curves are the estimated standard deviations and the discrete points are the absolute value of the errors between the nominal orbital elements and the estimated values. The figures show that the errors generally lie within the 1σ bound.

Another useful quantity is the normalized covariance matrix. This is generated using the relation

$$\hat{P}_{ij} = \frac{P_{ij}}{\sqrt{P_{ii}P_{jj}}} \quad .$$

It can be seen that the diagonal elements of $\hat{P}_{ij}$ will be unity while the off-diagonal elements range from zero to unity. A value of unity for $\hat{P}_{ij}$ indicates that δx_i and δx_j are linearly related while a value of zero indicates that their relationship is purely random. Examples of the normalized covariance matrix for tracking time of 6 and 48 hours for a six and seven dimension state vector are given in Tables 1 and 2, respectively.

V. Areas for Further Investigation

1) The motion of the earth was assumed to be a circular orbit with zero inclination and the earth's polar axis was assumed to be normally inclined to the orbital plane in order to avoid the transformation of $\underline{R}(t)$ from the earth-centered equatorial frame to the earth-centered ecliptic frame described previously. This transformation might be introduced for completeness.

2) No provision was made to take into account loss of tracking data due to occultation of the satellite by either earth or Mars. This could make a significant difference in the time needed to estimate the state vector, particularly if data near periapsis is lost.

3) The motion of the satellite about Mars was assumed to be essentially Keplerian in nature. For the orbits and tracking times discussed, this is a good assumption. However, for higher orbits (i.e., synchronous altitudes and above), solar perturbations may also exert a noticable effect. It should also be noted that the J_2 term in the planetary gravitational field gives rise to secular changes in ω and Ω. These changes may amount to about .05 - .2 deg/day for the orbits discussed and suggest that our estimate for these parameters be updated at weekly intervals. Alternatively, these secular changes in ω and Ω could be included in our equations of motion to allow longer periods of validity for our estimate. If this is done, the additional coordinate rotations described in Equation 8 must be included so that calculations may be performed in the planetary equatorial frame.

4) The random noise added to the simulated measurements was generated by the normal distribution pseudo-random noise generator included in the Univac 1108 Mathpack subroutine. The desired moments were zero mean and a standard deviation of

$$\sigma = .152.$$

These were generally accurate to about .02 for both the mean and the standard deviation. However, histograms plotted for distributions of 100 points showed that the distribution did not closely resemble the bell-shaped curve for a normal distribution. Often, a skewed, two-hump distribution resulted. In addition, plots of points in the sequence of their generation showed certain non-random patterns (e.g., every second or fourth point following a smooth curve for 30 or 40 points). This latter result violates our assumption of uncorrelated noise. The fact that the actual errors did, however, consistently lie near or within the one sigma bound indicates that this violation was not too serious. Still, a more accurate means of generating random noise with a normal distribution might be investigated.

5) In some instances (e.g., for the gravitational parameter μ) we have an a priori estimate of both a parameter and its statistics. These a priori statistics of the initial guess may be included to weight the initial guess for that parameter more heavily. This is done by changing Equation (15) to

$$P^{-1} = M^{-1} + H^T R^{-1} H$$

where

$$M = E[(\underline{x} - \overline{\underline{x}})(\underline{x} - \overline{\underline{x}})^T] \quad .$$

One effect of including the statistics of the initial elements would be to decrease the large standard deviations for short tracking times.

6) For a real measurement program Eq. (9) must be written to account for the light-time correction. That is, the measured Doppler shift is the difference between the signal frequency transmitted at t_o from $R(t_o)$ and that received at $R(t_2)$, this being a measure of the satellite velocity at time t_1, where $t_2 - t_1 \approx t_1 - t_o \approx D/c$ (c = velocity of light). Corrections for atmospheric refraction may also be made (see Ref. 3).

VI. **Conclusions**

The state vector of a planetary artificial satellite can be accurately determined using range-rate measurements taken from earth. The error estimates given by the covariance matrix provide a conservative upper bound for errors in the state estimation when the method of differential corrections is used with simulated noisy measurements.

The accuracy of the state estimation is a function both of the number of data points and the total tracking time. No rigorous attempt was made to optimize tracking time or data point spacing but a spacing of .5 hrs and a tracking time of 30-40 hrs yield good results for the cases simulated. The accuracy of the estimation for some state vector parameters decreased significantly when the gravitational parameter of the planet was added to the state vector.

For relatively eccentric orbits, the state estimation showed a fluctuation in accuracy with the same period as the orbit. This was caused by the higher rate of data influx near periapsis due to the higher angular velocity of the satellite. The accuracy in estimation of a and τ appeared to depend more

on the number of orbits tracked rather than on the tracking time. This was caused by the presence of constant or secular terms whose coefficients depended on the magnitude of the satellite mean motion. The accuracy of estimation of a, τ, and μ, as well as ω and Ω when μ is estimated, showed an increase as the eccentricity of the orbit increased.

W. B. Thompson for S.S.B.

1014-SSB-jan   S. S. Bayliss

BELLCOMM, INC.

REFERENCES

1. Optimal Programming, Estimation, and Control, A. E. Bryson, and Y. C. Ho, Harvard University, Cambridge, Massachusetts.

2. "Determination of Orbits of Planetary Artificial Satellites and Planetary Gravitational Fields," C. L. Greer and C. C. H. Tang, Bellcomm Technical Report TR-68-720-1, May 24, 1968.

3. "The Mariner IV Flight Path and Its Determination From Tracking Data," JPL Technical Report 32-1108, August 1, 1967, a) p. 3, b) p. 185, c) p. 38.

4. "TRW Space Data," TRW Systems Group, 1967, a) p. 110, b) pp. 8, 14-15.

5. "Evaluation of Space Navigation Techniques for Manned Mars Flyby Mission," Bellcomm Memorandum for File, J. E. Volonte, March 6, 1967.

6. "JPL Development Ephemeris Number 19," JPL Technical Report 32-1181, November 15, 1967, a) pp. 18-19, b) p. 38.

7. "Ephemerides of the Earth and Venus From Radar," D. O. Muhleman, Astronomical Journal, April, 1967.

8. "Astronomical Constants and Planetary Ephemerides Deduced from Radar and Optical Observations," M. E. Ash, I. I. Shapiro, W. B. Smith, Astronomical Journal, April, 1967.

APPENDIX A

Error Sources in the Measurement Function F

This appendix examines the principal sources of error that make up the total error σ (see Equation (17) in the text) in the measurement function F and derives typical one sigma values for their contribution to this total error.

1) Error in Tracking Station Location

Assume typical 1σ station location errors to be ± 30 m (Reference 3a) in the local geographic reference frame

$$x\text{-axis} = \text{North}$$

$$y\text{-axis} = \text{East}$$

$$z\text{-axis} = \text{down}.$$

For the earth, we have

$$R_E = 6378.16 \text{ km}$$

$$\omega_{ie} = 7.292 \ (10^{-5}) \text{ rad/sec} \ .$$

For a point on the earth's surface at latitude L, the velocity due to the earth's rotation is

$$V = R_E \omega_{ie} \ \cos L \ \ .$$

An error in location in the z-direction causes a velocity change of

$$\delta V_z = \omega_{ie} \ \cos L \ \delta z \ \ .$$

An error in the x-direction causes

$$\delta V_x = -\omega_{ie} \ \sin L \ \delta x \ \ .$$

An error in the y-direction causes no significant error in velocity. Combining these contributions, we get

$$\delta V = \sqrt{\delta V_x{}^2 + \delta V_z{}^2}$$

$$= \omega_{ie} \ \sqrt{\delta x^2 + \delta z^2} \ \ .$$

Since

$$\delta x = \delta z = 30 \text{ m} ,$$

we get

$$\delta V = .00308 \text{ m/sec} \quad (1\sigma \text{ error}) .$$

2) Error in Speed of Light

        Assume the 1σ error in the speed of light, c, to be
± 100 m/sec (Reference 4a). Using a two-way Doppler measurement
system, the relative velocity is given by

$$V_R = \frac{cF_d}{2F_o}$$

where

$$F_d = \text{Doppler shift}$$

$$F_o = \text{original frequency}$$

Thus,

$$\delta V_R = \frac{F_d}{2F_o} \delta c .$$

For

$$V_R = 10,000 \text{ m/sec}$$

$$F_o = 2200 \text{ MHz} ,$$

we get

$$F_d = 14,700 \text{ Hz}$$

Then

$$\delta V_R = .000334 \text{ m/sec}$$

3) Frequency Measurement Errors

        Reference 5 gives two-way Doppler tracking errors
as .001 m/sec.

        Reference 3b gives Doppler measurement accuracies
as being of the order of .01 Hz or lower. This corresponds
to a velocity error of .00068 m/sec.

4) Ephemeris Errors

        Reference 6a gives the 1σ errors in the JPL fitted
planetary ephemerides for Mars and the earth-moon system
in an ecliptic reference frame as

	Earth-Moon	Mars
δx	35 km	19.2 km
δy	34.7 km	13.8 km
δz	21.1 km	8.35 km

        Errors in the tangential direction will have only
a negligible effect on the measurement function through changes
in the station-satellite direction. Errors in the radial
direction will have a significant effect on the planetary
velocity and will be examined further in the next section.
For estimation purposes, we assume the radial position error
to be 17 km for Mars and 35 km for earth. Note that this does
not include the error in the A.U.

        Reference 6b gives the plots of the velocity residuals
for the ephemeris calculations in the JPL Development Ephemeris.
From inspection, it would appear that a 1σ figure of .03 m/sec
for earth and .015 m/sec for Mars are representative values.
We assume this figure includes effects of radial position errors.

5) Error in the Astronomical Unit

        Reference 3c gives two references for values of the
A.U. (References 7 and 8). The values given are

$$AU = 149,598,000 \pm 100 \text{ km} \qquad \text{(Reference 7)}$$

$$AU = 149,597,892 \pm 100 \text{ km} \qquad \text{(Reference 8)}$$

Since ephemeris position is given in terms of the A.U.,
an error in the A.U. leads to an error in planetary position.
Assuming average radial distances for earth and Mars of

$$r_E = 1.0 \text{ A.U.}$$

$$r_M = 1.52 \text{ A.U. },$$

we get a radial error of 100 km in the position of earth and
152 km in the position of Mars. Using the energy equation

$$V^2 = \mu[\frac{2}{R} - \frac{1}{a}]$$

we see

$$\delta V = -\frac{\mu}{VR^2} \ \delta R \ .$$

The average values for R and V are given in Reference 4b as

	Earth	Mars
R	$1.496(10^{11})$ m	$2.28(10^{11})$ m
V	29,770 m/sec	24,020 m/sec .

The value for the gravitational parameter of the sun is given as

$$\mu = 1.327(10^{20}) \ m^3/sec^2 \ .$$

Using these values, we get

$$\delta V = \pm.0199 \ m/sec$$

for the earth and

$$\delta V = \pm.0162 \ m/sec$$

for Mars due to error in the A.U.

6) Summary of Errors

From Sections 1-5, we had the following errors:

Source	Value
Station Location	.00308 m/sec
Speed of Light	.000334 m/sec
Frequency Measurement	.00068 m/sec
Ephemeris	
Earth	.03 m/sec
Mars	.015 m/sec
A.U.	
Earth	.0199 m/sec
Mars	.0162 m/sec

Taking the square root of the sum of the squares of these values, we get

$$\delta V = .0423 \text{ m/sec}$$

$$= .152 \text{ km/hr} \quad (1\sigma \text{ error}) .$$

This roughly compares with the 1σ values of $\pm.03$ m/sec used in the JPL report on Mariner IV tracking analysis (Reference 3).

       The RMS error was computed assuming uncorrelated error sources. Obviously some of the errors described are correlated. Thus the value of .0423 m/sec should be an upper bound on the actual error. This is true so long as the heliocentric angle between Earth and Mars is less than 90°, since the A.U. errors in heliocentric velocity are correlated and should be added vectorially. For example, at 0° heliocentric angle the relative velocity error should be $\pm.0037$ m/sec, while at 180° it should be $\pm.0361$ m/sec.

APPENDIX B

Partials of Measurement Function

From Equation (10), we had the measurement function as:

$$F(\underline{x},t) = \dot{\underline{\rho}}(x,t) \cdot \hat{\underline{\rho}}(x,t) \tag{B1}$$

where

$$\underline{\rho} = \underline{r}(\underline{x},t) - \underline{D}(t) - \underline{R}(t) \tag{B2}$$

thus

$$\frac{\partial F}{\partial \underline{x}} = \frac{\partial \dot{\underline{\rho}}}{\partial \underline{x}} \cdot \hat{\underline{\rho}} + \dot{\underline{\rho}} \cdot \frac{\partial \hat{\underline{\rho}}}{\partial \underline{x}} \tag{B3}$$

Since

$$\hat{\underline{\rho}} = \frac{\underline{\rho}}{|\underline{\rho}|}$$

we get

$$\frac{\partial \hat{\underline{\rho}}}{\partial \underline{x}} = \frac{1}{|\underline{\rho}|} \frac{\partial \underline{\rho}}{\partial \underline{x}} - \frac{\partial |\underline{\rho}|}{\partial \underline{x}} \frac{\underline{\rho}}{|\underline{\rho}|^2} \tag{B4}$$

Also, we may show

$$\frac{\partial |\underline{\rho}|}{\partial \underline{x}} = \hat{\underline{\rho}} \cdot \frac{\partial \underline{\rho}}{\partial \underline{x}}$$

Thus

$$\frac{\partial F}{\partial \underline{x}} = \frac{\partial \dot{\underline{\rho}}}{\partial \underline{x}} \cdot \hat{\underline{\rho}} + \dot{\underline{\rho}} \cdot \left[\frac{\partial \underline{\rho}}{\underline{x}} \frac{1}{|\underline{\rho}|} - \frac{\underline{\rho}}{|\underline{\rho}|^2} \left(\hat{\underline{\rho}} \cdot \frac{\partial \underline{\rho}}{\partial \underline{x}} \right) \right] \tag{B5}$$

From (B2), we see

$$\frac{\partial \dot{\underline{\rho}}}{\partial \underline{x}} = \frac{\partial \dot{\underline{r}}}{\partial \underline{x}} \quad ; \quad \frac{\partial \underline{\rho}}{\partial \underline{x}} = \frac{\partial \underline{r}}{\partial \underline{x}}$$

Thus

$$\frac{\partial F}{\partial \underline{x}} = \frac{\partial \dot{\underline{r}}}{\partial \underline{x}} \cdot \hat{\underline{\rho}} + \frac{\dot{\rho}}{|\underline{\rho}|} \cdot \left[\frac{\partial \underline{r}}{\partial \underline{x}} - \hat{\underline{\rho}} \left(\hat{\underline{\rho}} \cdot \frac{\partial \underline{r}}{\partial \underline{x}} \right) \right]$$

$$= \frac{\partial \dot{\underline{r}}}{\partial \underline{x}} \cdot \hat{\underline{\rho}} + \frac{1}{|\underline{\rho}|} \left[\left(\dot{\underline{\rho}} \cdot \frac{\partial \underline{r}}{\partial \underline{x}} \right) - \left(\dot{\underline{\rho}} \cdot \hat{\underline{\rho}} \right) \left(\hat{\underline{\rho}} \cdot \frac{\partial \underline{r}}{\partial \underline{x}} \right) \right]$$

$$= \frac{\partial \dot{\underline{r}}}{\partial \underline{x}} \cdot \hat{\underline{\rho}} + \frac{1}{|\underline{\rho}|} \left[\left(\dot{\underline{\rho}} \cdot \frac{\partial \underline{r}}{\partial \underline{x}} \right) - \left(\hat{\underline{\rho}} \cdot \frac{\partial \underline{r}}{\partial \underline{x}} \right) F \right]$$

Thus

$$\frac{\partial F}{\partial \underline{x}} = \frac{\partial \dot{\underline{r}}}{\partial \underline{x}} \cdot \hat{\underline{\rho}} + \frac{\partial \underline{r}}{\partial \underline{x}} \cdot \left[\frac{\dot{\underline{\rho}}}{|\underline{\rho}|} - \frac{\hat{\underline{\rho}}}{|\underline{\rho}|} F \right] \qquad (B6)$$

The quantities $\hat{\underline{\rho}}$, $\dot{\underline{\rho}}$, and $|\underline{\rho}|$ are evaluated using Equation (B2) with the nominal values of $\underline{x}$. The values for $\frac{\partial \underline{r}}{\partial \underline{x}}$ and $\frac{\partial \dot{\underline{r}}}{\partial \underline{x}}$ can be calculated in the following manner.

From Equations (5) and (6), it can be shown

$$\underline{r} = |\underline{r}| \begin{bmatrix} \cos \Omega \cos(\omega+f) - \sin \Omega \sin(\omega+f) \cos i \\ \sin \Omega \cos(\omega+f) + \cos \Omega \sin(\omega+f) \cos i \\ \sin(\omega+f) \sin i \end{bmatrix}$$

$$\dot{\underline{r}} = N \begin{bmatrix} -\cos \Omega(\sin(\omega+f) + e \sin \omega) - \sin \Omega \cos i (\cos(\omega+f) + e \cos \omega) \\ -\sin \Omega(\sin(\omega+f) + e \sin \omega) + \cos \Omega \cos i (\cos(\omega+f) + e \cos \omega) \\ (\cos(\omega+f) + e \cos \omega) \sin i \end{bmatrix}$$

where

$$|\underline{r}| = \frac{a(1-e^2)}{1+e \cos f} \quad ; \qquad N = \left[\frac{\mu}{a(1-e^2)} \right]^{1/2}$$

Using these equations, the partials may be shown to be

$$\frac{\partial \underline{r}}{\partial \alpha} = \begin{bmatrix} \frac{\partial |\underline{r}|}{\partial \alpha} x_2 + |\underline{r}| \frac{\partial x_2}{\partial f} \frac{\partial f}{\partial \alpha} \\[2em] \frac{\partial |\underline{r}|}{\partial \alpha} y_2 + |\underline{r}| \frac{\partial y_2}{\partial f} \frac{\partial f}{\partial \alpha} \\[2em] \frac{\partial |\underline{r}|}{\partial \alpha} z_2 + |\underline{r}| \frac{\partial z_2}{\partial f} \frac{\partial f}{\partial \alpha} \end{bmatrix} (\alpha = a,e,\tau,\mu) \qquad (B7)$$

where

$$\hat{\underline{r}}^T = \frac{\underline{r}^T}{|\underline{r}|} = [x_2, y_2, z_2]$$

$$\frac{\partial \hat{\underline{r}}}{\partial f} = \begin{bmatrix} -\cos \Omega \sin(\omega+f) - \sin \Omega \cos(\omega+f) \cos i \\ -\sin \Omega \sin(\omega+f) + \cos \Omega \cos(\omega+f) \cos i \\ \cos(\omega+f) \sin i \end{bmatrix}$$

$$\frac{\partial |\underline{r}|}{\partial a} = \frac{|\underline{r}|}{a} + |\underline{r}| \frac{e \sin f}{1+e \cos f} \frac{\partial f}{\partial a}$$

$$\frac{\partial |\underline{r}|}{\partial e} = -|\underline{r}| \left(\frac{2e}{1-e^2}\right) - |\underline{r}| \frac{\cos f}{1+e \cos f} + |\underline{r}| \frac{e \sin f}{1+e \cos f} \frac{\partial f}{\partial e}$$

$$\frac{\partial |\underline{r}|}{\partial \tau} = |\underline{r}| \frac{e \sin f}{1+e \cos f} \frac{\partial f}{\partial \tau}$$

$$\frac{\partial |\underline{r}|}{\partial \mu} = |\underline{r}| \frac{e \sin f}{1+e \cos f} \frac{\partial f}{\partial \mu}$$

$$\frac{\partial f}{\partial a} = -\frac{3}{2} \; \frac{N^3}{\mu a} \; (1+e \cos f)^2 (t-\tau)$$

$$\frac{\partial f}{\partial e} = \frac{\sin f}{(1-e^2)} \; (2+e \cos f)$$

$$\frac{\partial f}{\partial \tau} = -\frac{N^3}{\mu} \; (1+e \cos f)^2$$

$$\frac{\partial f}{\partial \mu} = \frac{1}{2} \; \frac{N^3}{\mu^2} \; (1+e \cos f)^2 \; (t-\tau)$$

The remaining partials are

$$\frac{\partial \underline{r}}{\partial \Omega} = |\underline{r}| \begin{bmatrix} -\sin \Omega \cos(\omega+f) - \cos \Omega \sin(\omega+f) \cos i \\ \cos \Omega \cos(\omega+f) - \sin \Omega \sin(\omega+f) \cos i \\ 0 \end{bmatrix} \tag{B8}$$

$$\frac{\partial \underline{r}}{\partial \omega} = |\underline{r}| \begin{bmatrix} -\cos \Omega \sin(\omega+f) - \sin \Omega \cos(\omega+f) \cos i \\ -\sin \Omega \sin(\omega+f) + \cos \Omega \cos(\omega+f) \cos i \\ \cos(\omega+f) \sin i \end{bmatrix} \tag{B9}$$

$$\frac{\partial \underline{r}}{\partial i} = |\underline{r}| \begin{bmatrix} \sin \Omega \sin(\omega+f) \sin i \\ -\cos \Omega \sin(\omega+f) \sin i \\ \sin(\omega+f) \cos i \end{bmatrix} \tag{B10}$$

For the partials of $\dot{\underline{r}}$ with respect to $\underline{x}$, we have

$$\frac{\partial \dot{\underline{r}}}{\partial \alpha} = \frac{\partial N}{\partial \alpha} \; \frac{\dot{\underline{r}}}{N} - \frac{N}{|\underline{r}|} \; \underline{r} \; \frac{\partial f}{\partial \alpha} \qquad (\alpha = a, \tau, \mu) \tag{B11}$$

where

$$\frac{\partial N}{\partial a} = - \frac{N}{2a}$$

$$\frac{\partial N}{\partial \mu} = \frac{N}{2\mu}$$

$$\frac{\partial N}{\partial \tau} = 0$$

$$\frac{\partial \dot{\underline{r}}}{\partial e} = \frac{e}{1-e^2} \dot{\underline{r}} - \frac{\underline{r}}{|\underline{r}|} \frac{N \partial f}{\partial e} + N T \qquad (B12)$$

where

$$T = \begin{bmatrix} -\cos \Omega \sin \omega - \sin \Omega \cos i \cos \omega \\ -\sin \Omega \sin \omega + \cos \Omega \cos i \cos \omega \\ \cos \omega \sin i \end{bmatrix}$$

$$\frac{\partial \dot{\underline{r}}}{\partial i} = N \begin{bmatrix} \sin \Omega \sin i(\cos(\omega+f) + e \cos \omega) \\ -\cos \Omega \sin i(\cos(\omega+f) + e \cos \omega) \\ \cos i(\cos(\omega+f) + e \cos \omega) \end{bmatrix} \qquad (B13)$$

$$\frac{\partial \dot{\underline{r}}}{\partial \omega} = N \begin{bmatrix} -\cos \Omega(\cos(\omega+f) + e \cos \omega) + \sin \Omega \cos i(\sin(\omega+f) + e \sin \omega) \\ -\sin \Omega(\cos(\omega+f) + e \cos \omega) - \cos \Omega \cos i(\sin(\omega+f) + e \sin \omega) \\ -(\sin(\omega+f) + e \sin \omega) \sin i \end{bmatrix}$$

$$\frac{\partial \dot{\underline{r}}}{\partial \Omega} = N \begin{bmatrix} \sin \Omega(\sin(\omega+f) + e \sin \omega) - \cos \Omega \cos i(\cos(\omega+f) + e \cos \omega) \\ -\cos \Omega(\sin(\omega+f) + e \sin \omega) - \sin \omega \cos i(\cos(\omega+f) + e \cos \omega) \\ 0 \end{bmatrix}$$

(B15)

Equations (B6) to (B15) allow us to calculate the vector $\frac{\partial F}{\partial \underline{x}} (\underline{\bar{x}}, t)$.

f = TRUE ANOMALY
ω = ARGUMENT OF PERIAPSIS
Ω = LONGITUDE OF ASCENDING NODE
i = INCLINATION OF ORBIT
A = VERNAL EQUINOX OF EARTH
N = ASCENDING NODE
π = PERIAPSIS
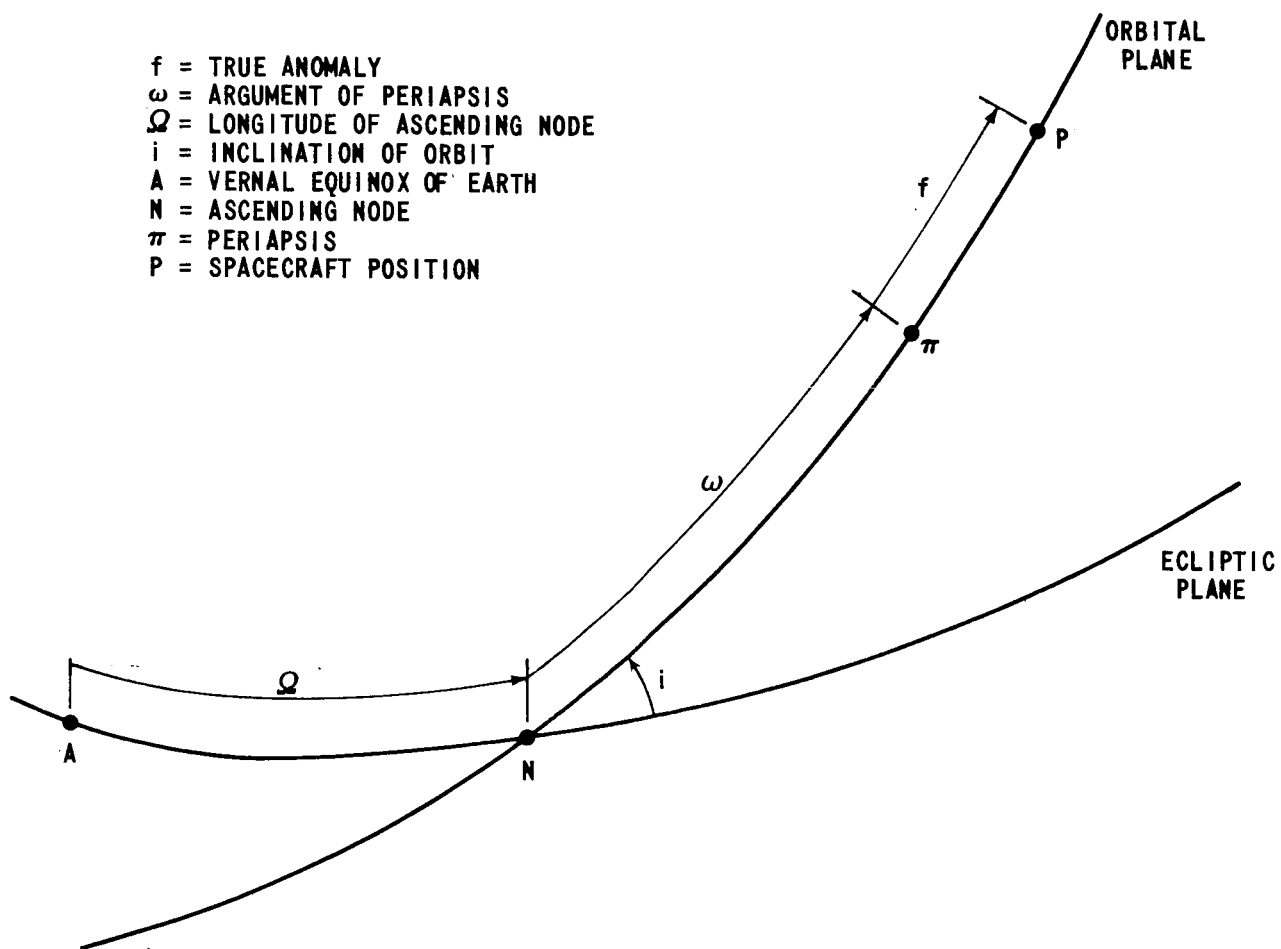P = SPACECRAFT POSITION

ORBITAL PLANE

ECLIPTIC PLANE

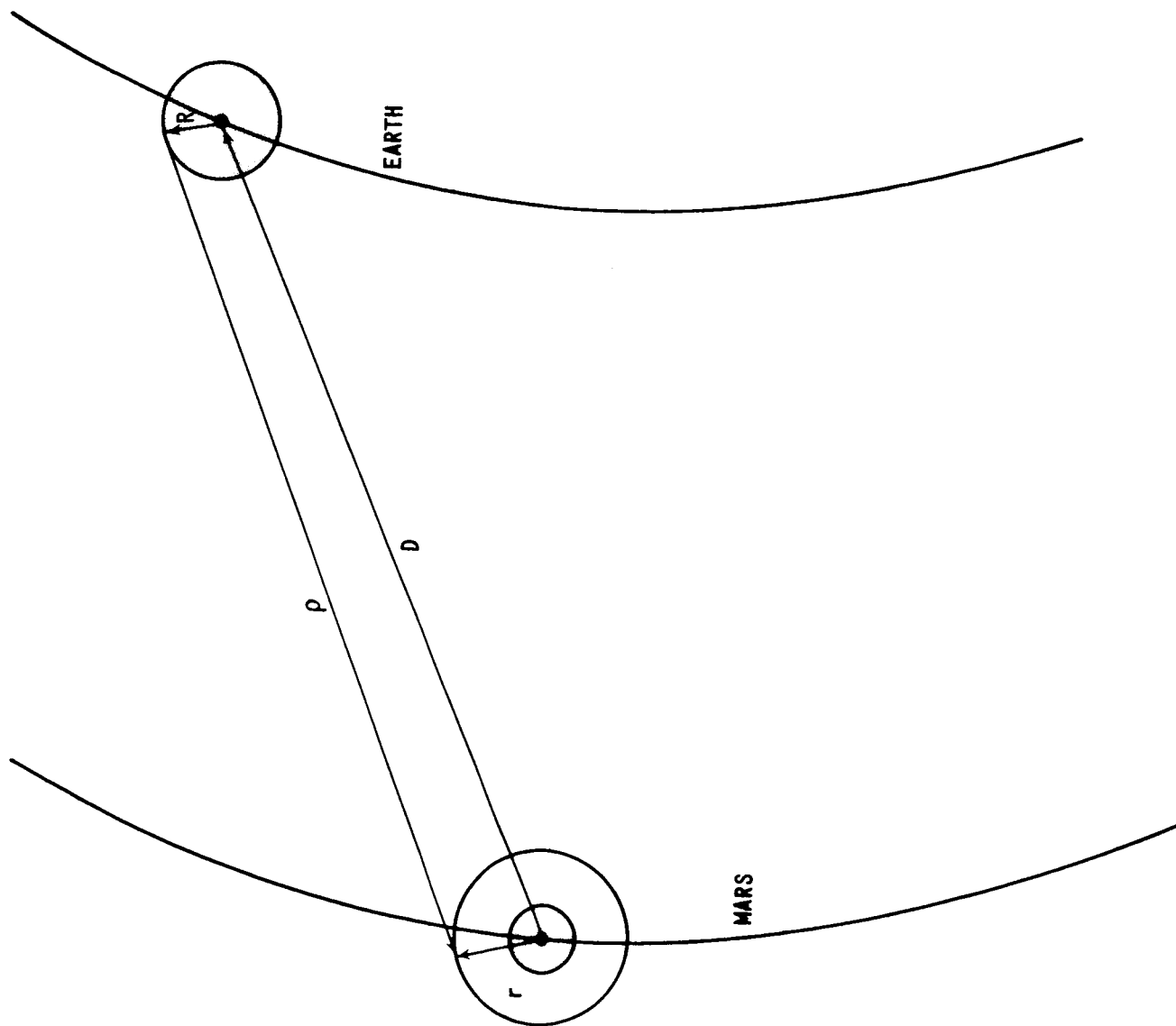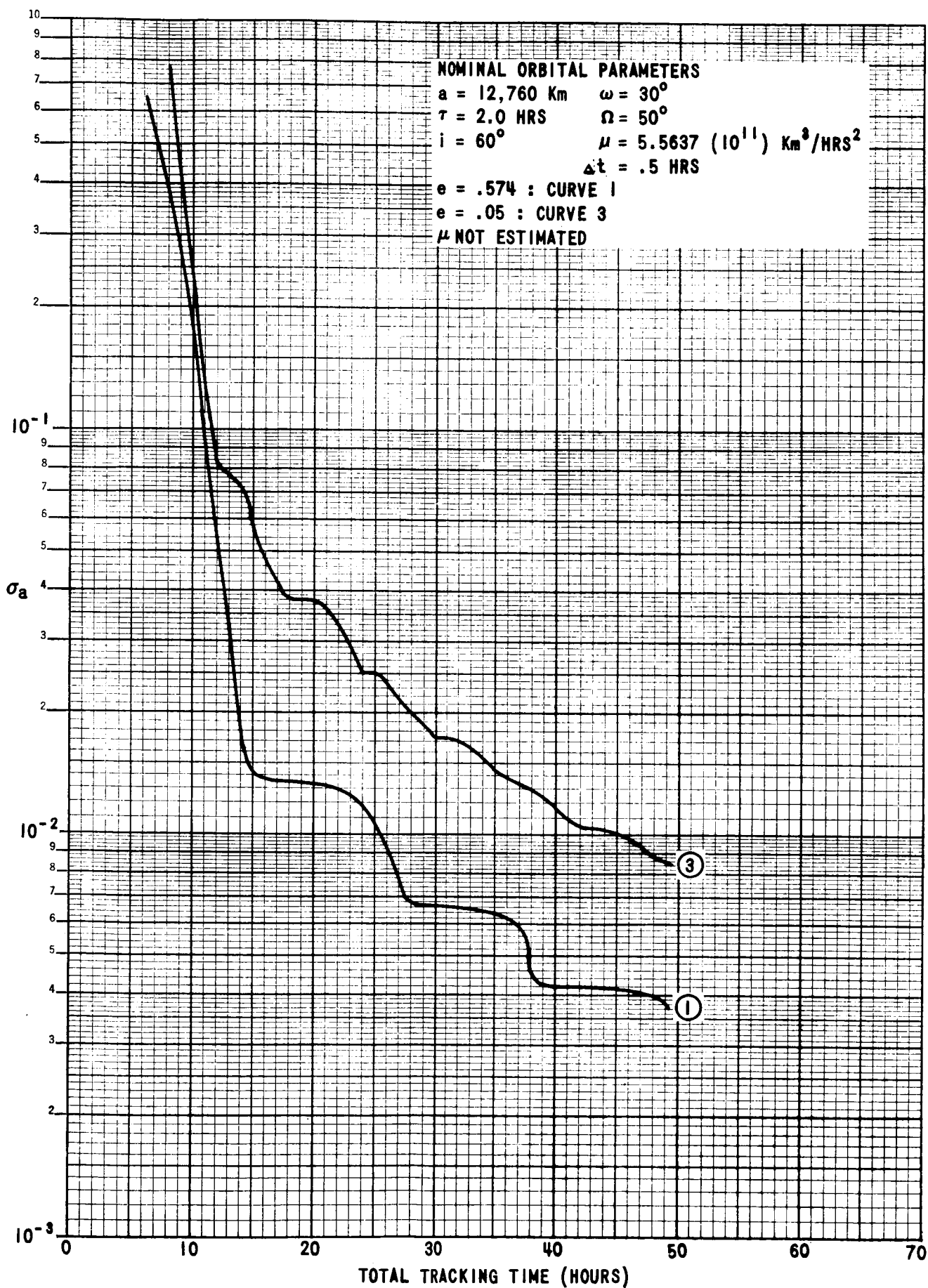FIGURE I - GEOMETRY OF ANGLE VARIABLES

FIGURE 2 - TRACKING GEOMETRY
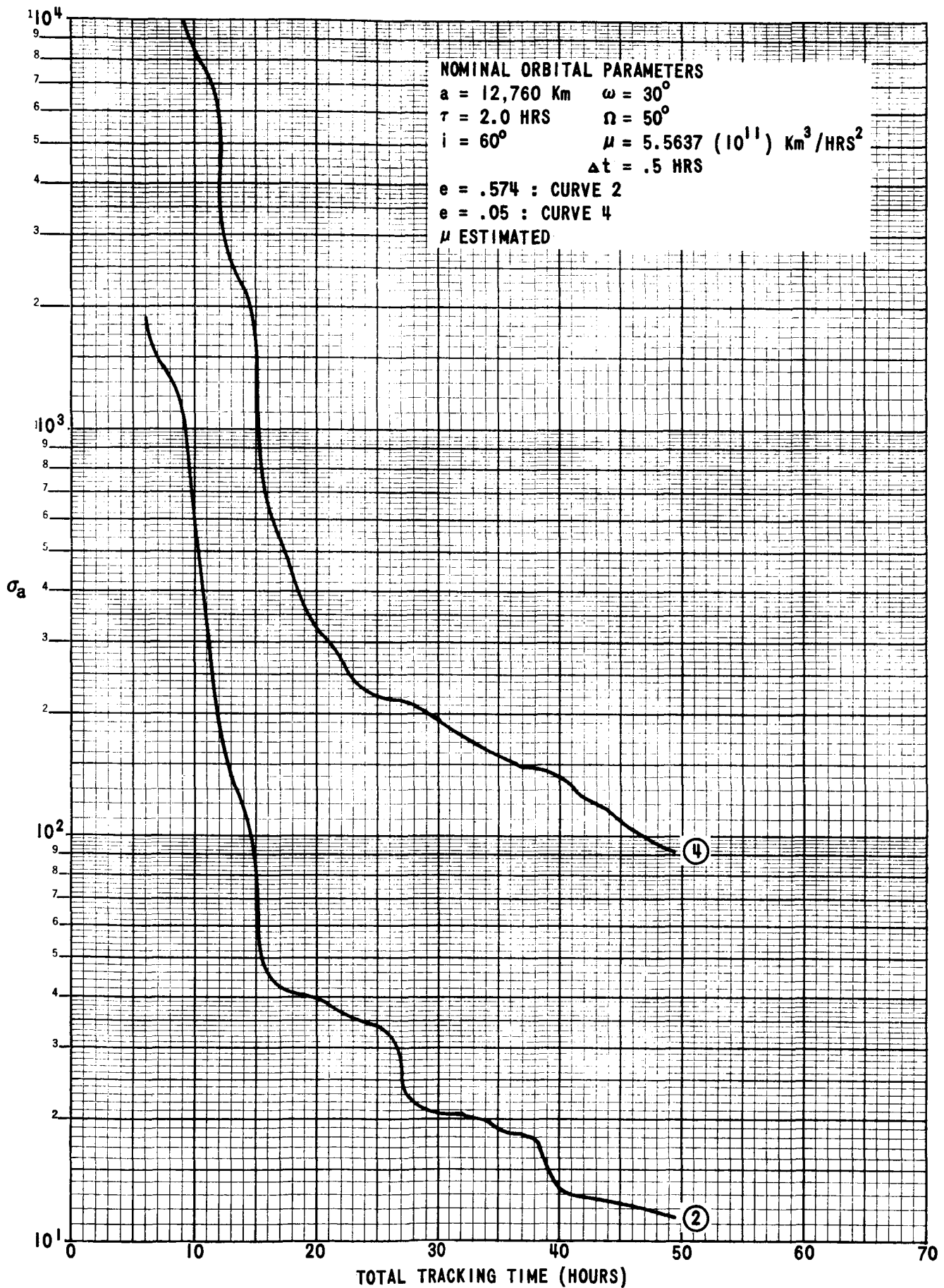
FIGURE 3 - STANDARD DEVIATION OF a VS TRACKING TIME

FIGURE 4 – STANDARD DEVIATION OF a VS TRACKING TIME

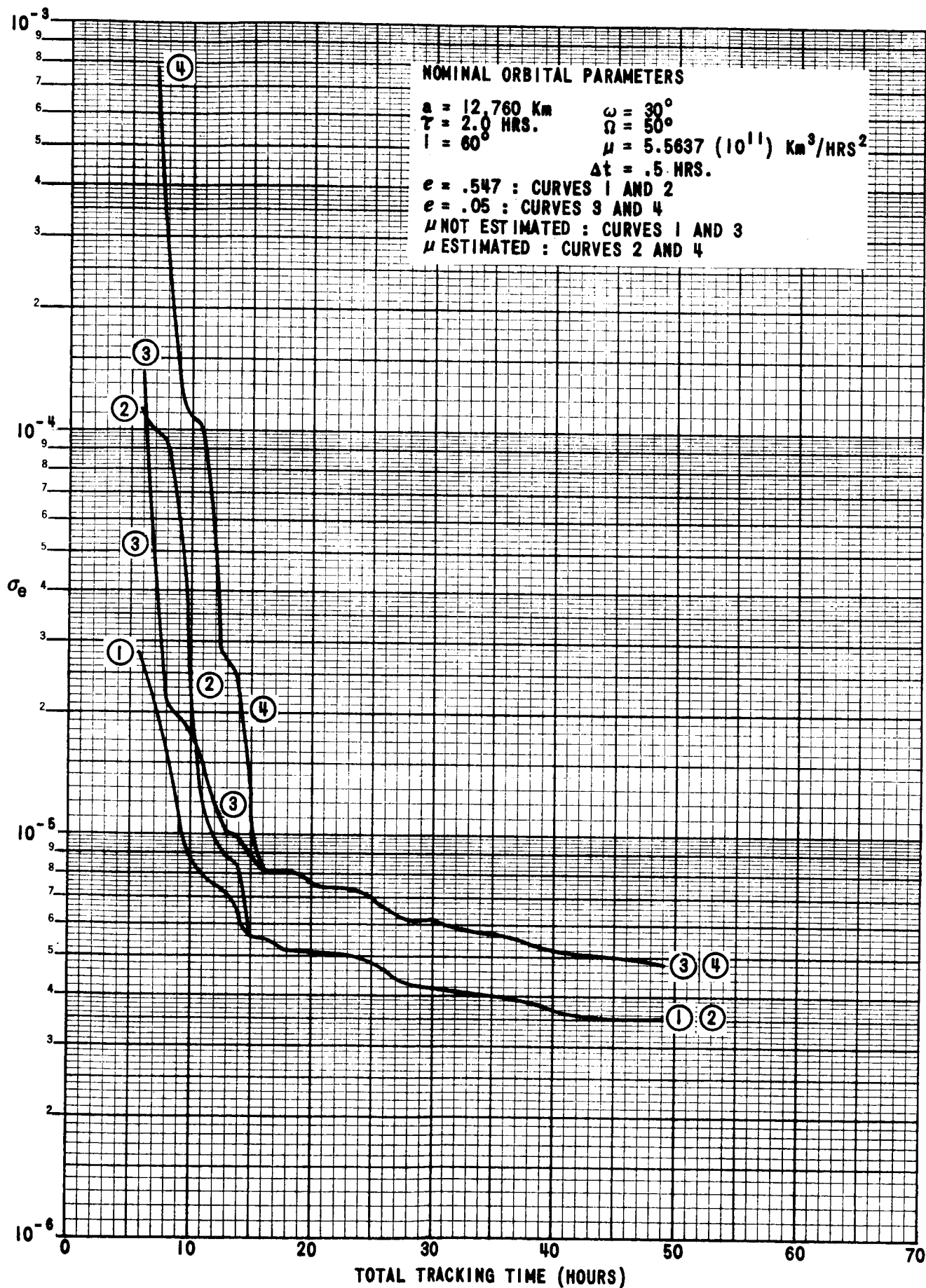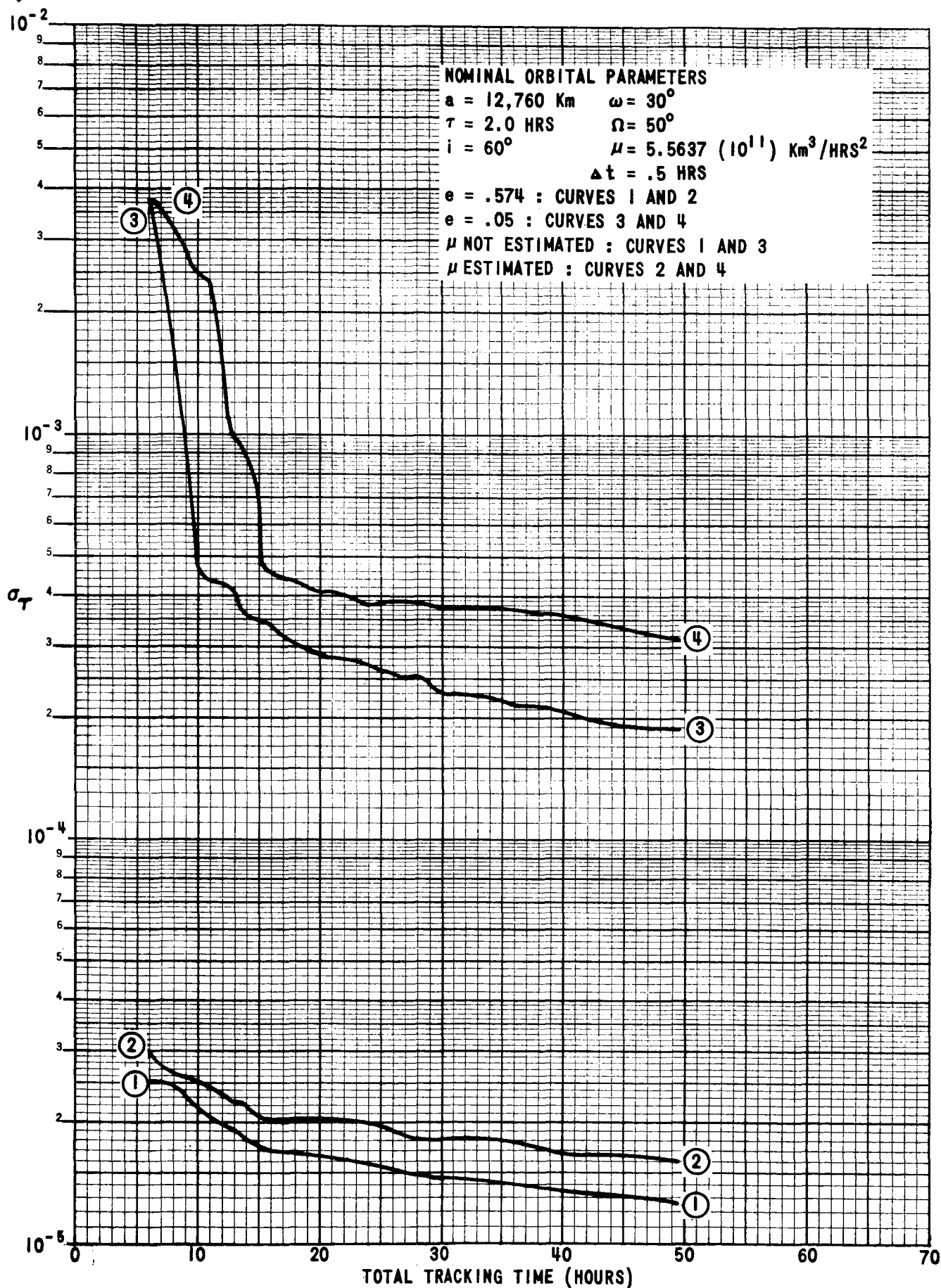FIGURE 5 - STANDARD DEVIATION OF e VS TRACKING TIME

FIGURE 6 - STANDARD DEVIATION OF τ VS TRACKING TIME

NOMINAL ORBITAL PARAMETERS
a = 12,760 Km ω = 30°
τ = 2.0 HRS Ω = 50°
i = 60° μ = 5.5637 (10^{11}) Km^3/HRS^2
Δt = .5 HRS
e = .574 : CURVES 1 AND 2
e = .05 : CURVES 3 AND 4
NOT ESTIMATED : CURVES 1 AND 3
ESTIMATED : CURVES 2 AND 4
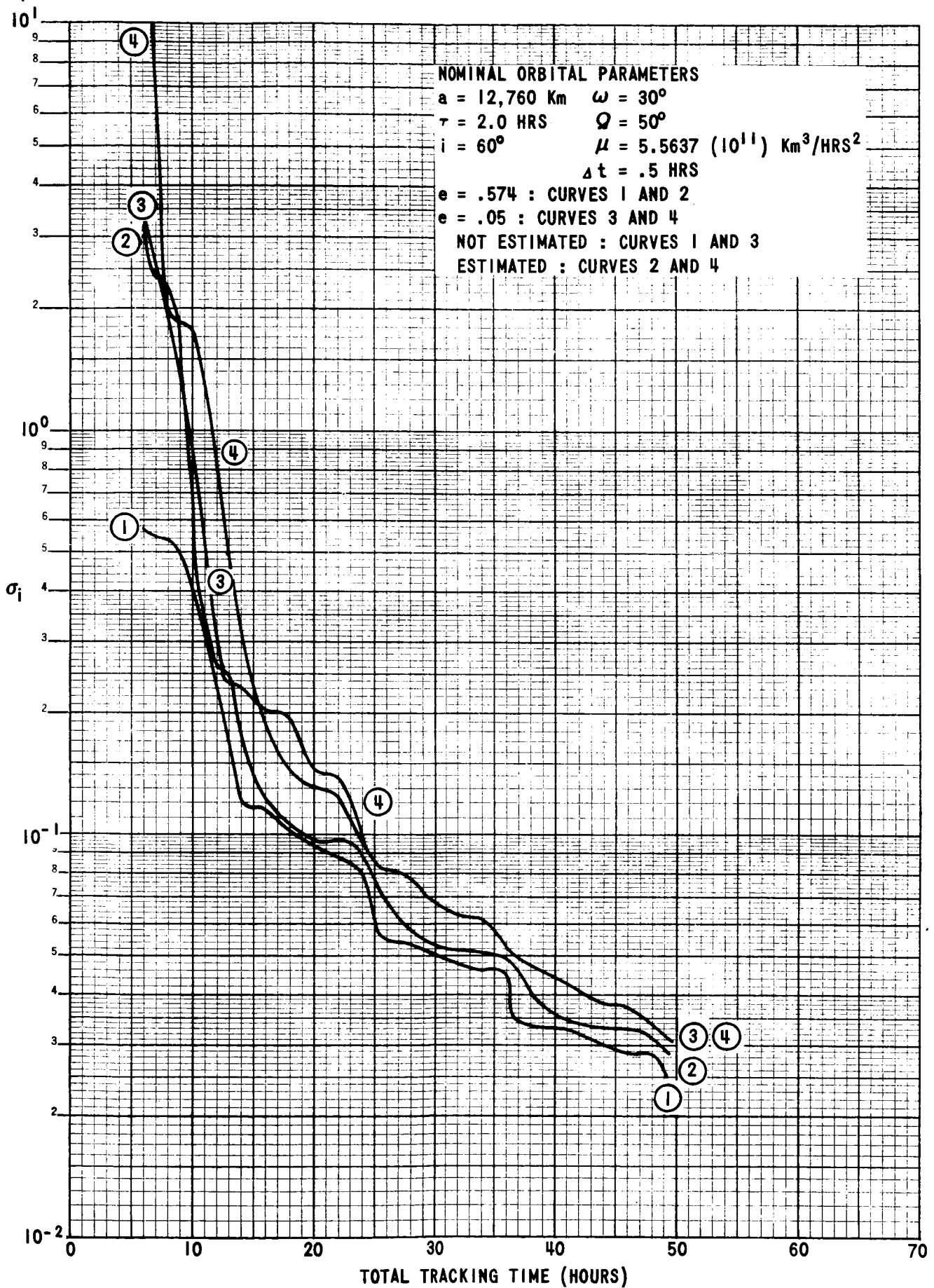
FIGURE 7 - STANDARD DEVIATION OF i VS TRACKING TIME

NOMINAL ORBITAL PARAMETERS

$a = 12,760$ Km $\omega = 30°$
$\tau = 2.0$ HRS. $\Omega = 50°$
$i = 60°$ $\mu = 5.5637 \ (10^{11}) \ Km^3/HRS^2$
    $\Delta t = .5$ HRS.
$e = .574$: CURVES 1 AND 2
$e = .05$: CURVES 3 AND 4
μ NOT ESTIMATED : CURVES 1 AND 3
μ ESTIMATED : CURVES 2 AND 4

TOTAL TRACKING TIME (HOURS)
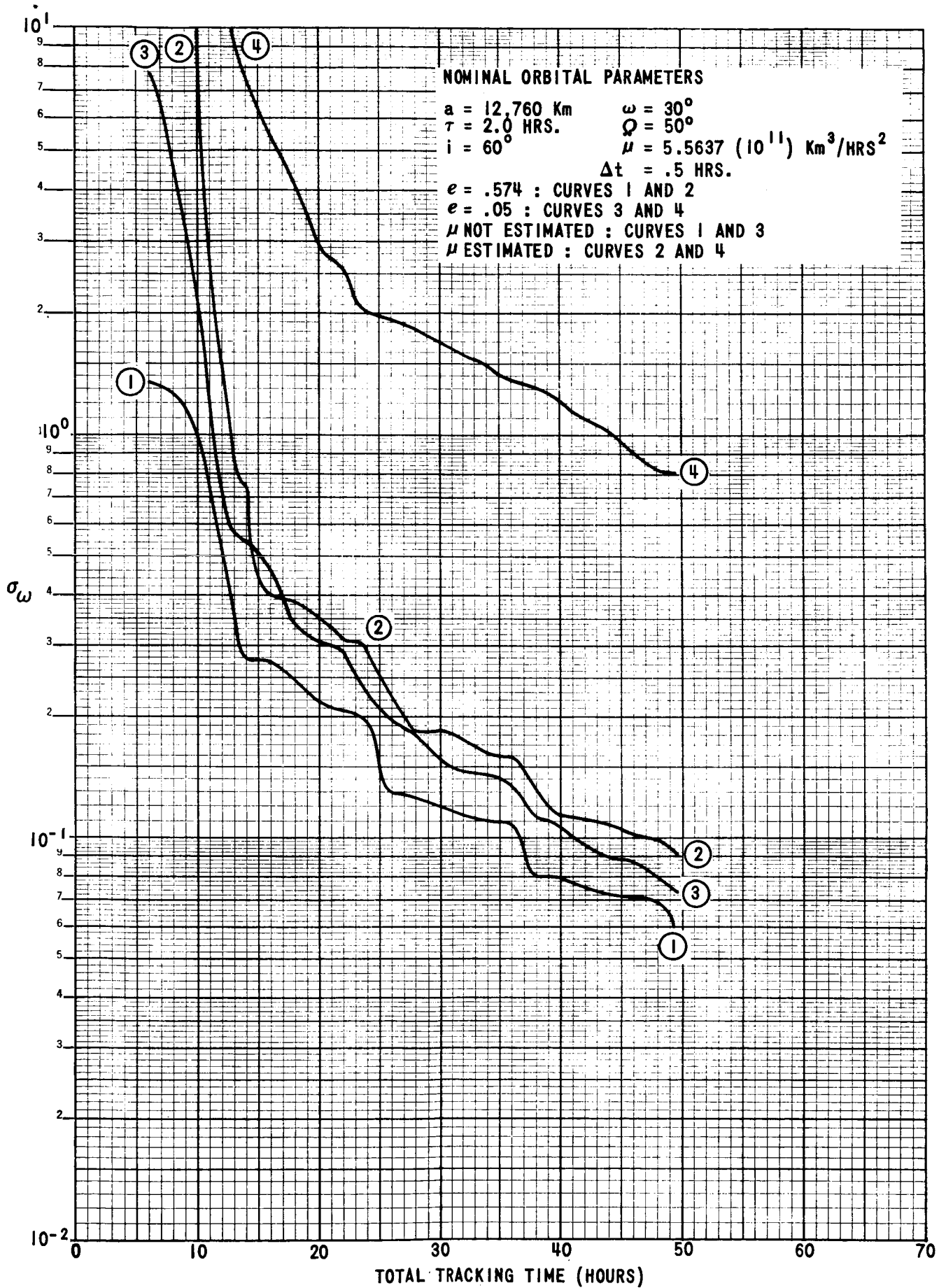
FIGURE 8 - STANDARD DEVIATION OF ω VS TRACKING TIME

NOMINAL ORBITAL PARAMETERS

$a = 12,760$ Km $\quad \omega = 30°$
$\tau = 2.0$ HRS $\quad \Omega = 50°$
$i = 60°$ $\qquad \mu = 5.5637 \ (10^{11}) \ Km^3/HRS^2$
$\qquad\qquad \Delta t = .5$ HRS
$e = .574$: CURVES 1 AND 2
$e = .05$: CURVES 3 AND 4
μ NOT ESTIMATED : CURVES 1 AND 3
μ ESTIMATED : CURVES 2 AND 4

TOTAL TRACKING TIME (HOURS)
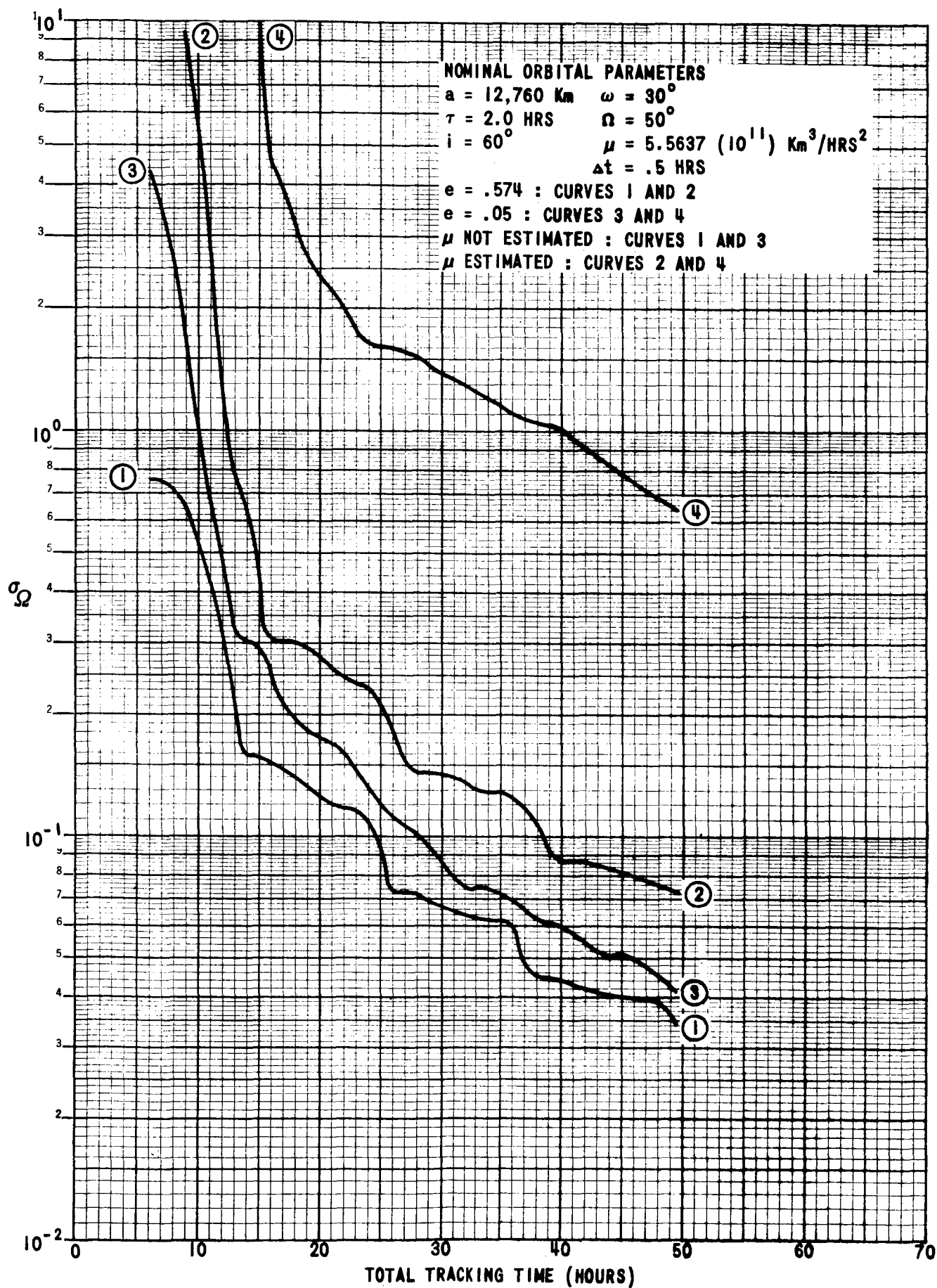
FIGURE 9 — STANDARD DEVIATION OF Ω VS TRACKING TIME

NOMINAL ORBITAL PARAMETERS

$a = 12,760$ Km $\omega = 30°$

$\tau = 2.0$ HRS $\Omega = 50°$

$i = 60°$ $\mu = 5.5637 \ (10^{11}) \ \text{Km}^3/\text{HRS}^2$

$\Delta t = .5$ HRS

$e = .574$: CURVE 2

$e = .05$: CURVE 4
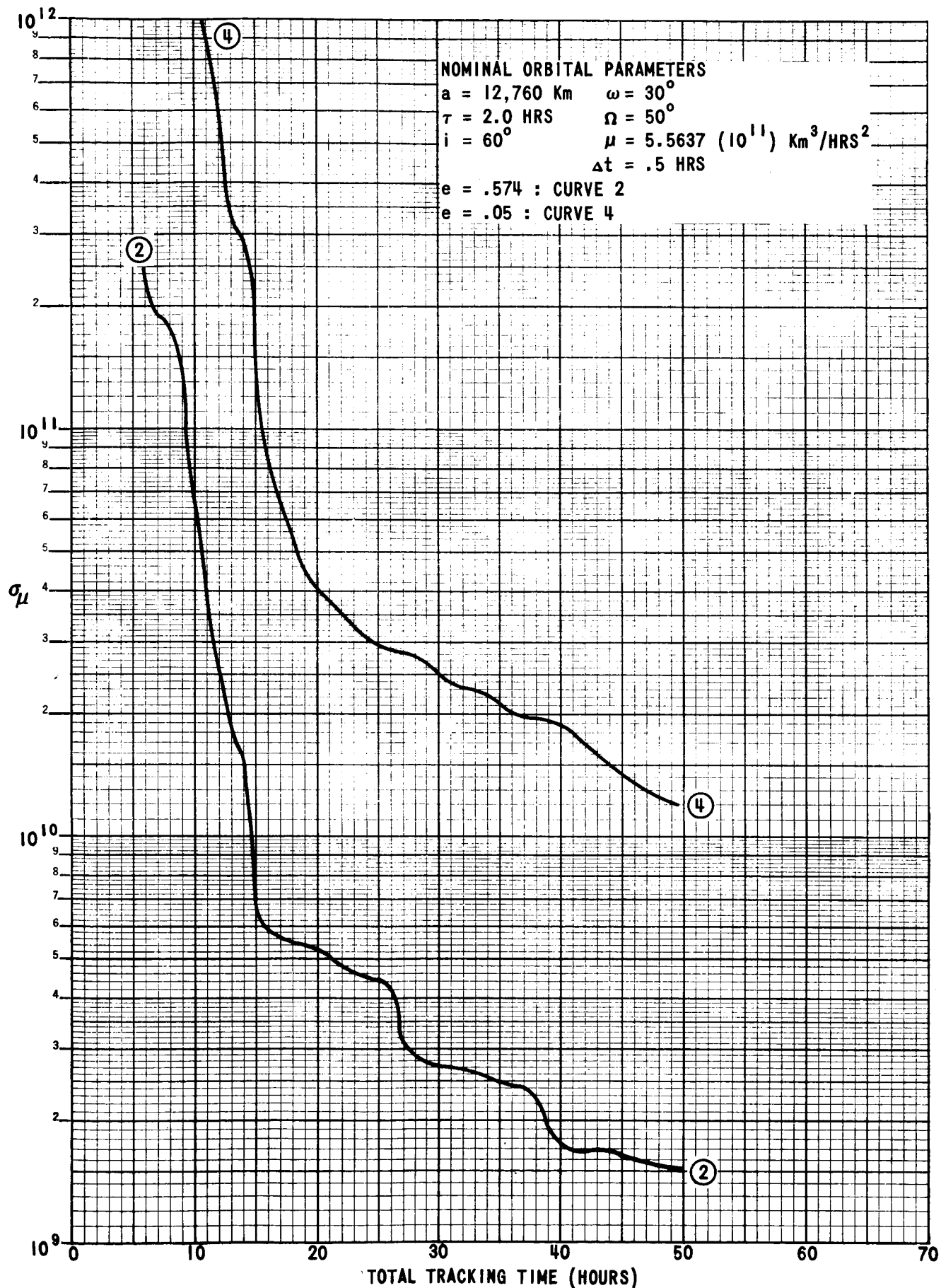
FIGURE 10 - STANDARD DEVIATION OF μ VS TRACKING TIME

NOMINAL ORBITAL PARAMETERS
$a = 12,760$ Km $I = 60°$
$e = .574$ $\omega = 30°$
$\tau = 2.0$ HRS $\Omega = 50°$
                  $\mu = 5.5673 \ (10^{11}) \ Km^3/HRS^2$
$\Delta t = .5$ HRS : CURVE 1
$\Delta t = .1$ HRS : CURVE 5
$\Delta t = 1.0$ HRS: CURVE 6
μ NOT ESTIMATED

σ_a

TOTAL TRACKING TIME (HOURS)
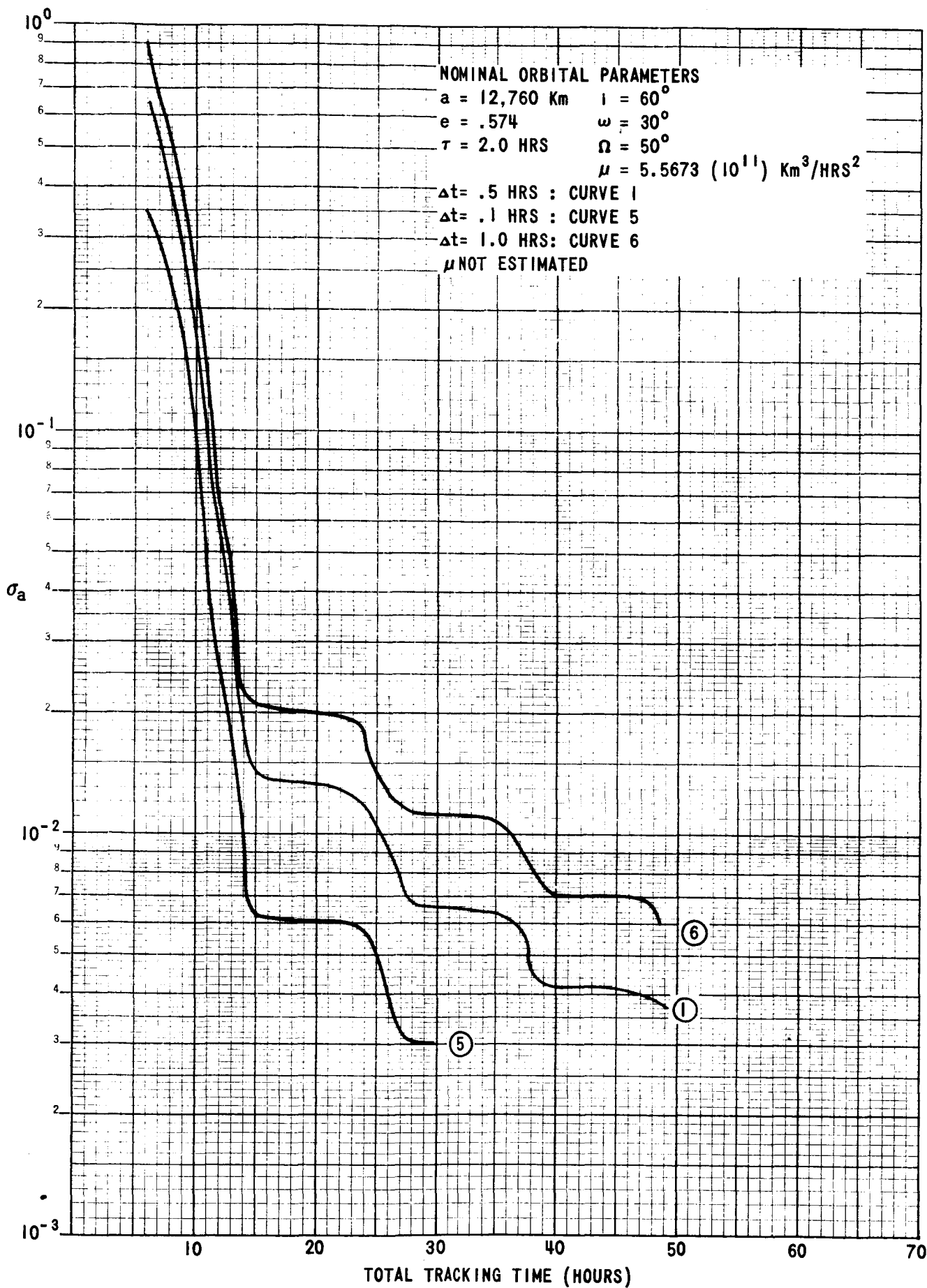
FIGURE 11 – STANDARD DEVIATION OF a VS TRACKING TIME

NOMINAL ORBITAL PARAMETERS

$a = 12,760$ Km $\quad i = 60°$

$e = .574 \quad\quad \omega = 30°$

$\tau = 2.0$ HRS $\quad \Omega = 50°$

$\mu = 5.5673 \ (10^{11}) \ Km^3/HRS^2$

$\Delta t = .5$ HRS : CURVE 1

$\Delta t = .1$ HRS : CURVE 5

$\Delta t = 1.0$ HRS: CURVE 6

μ NOT ESTIMATED

σ_e

TOTAL TRACKING TIME (HOURS)
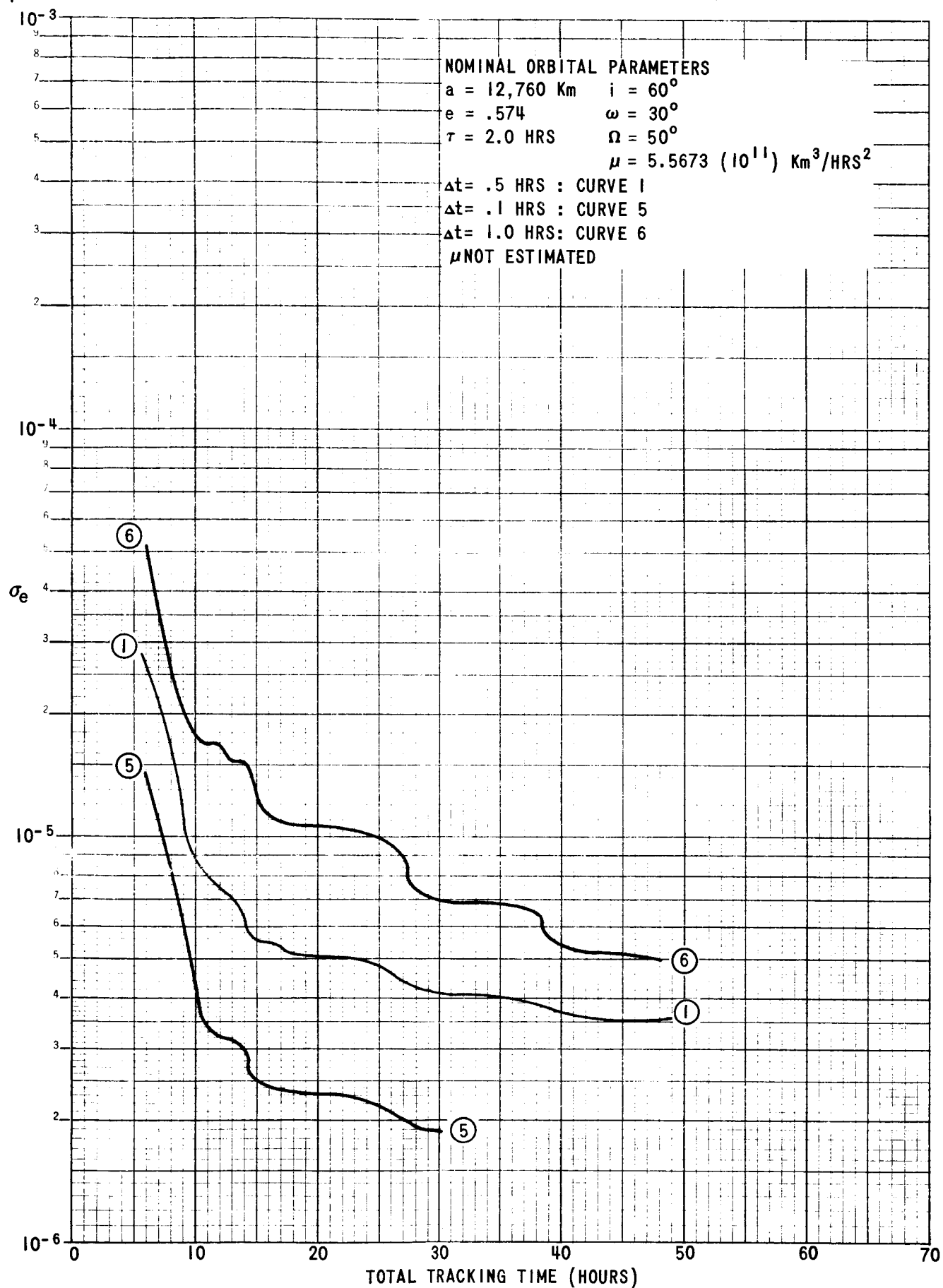
FIGURE 12 − STANDARD DEVIATION OF e VS TRACKING TIME

NOMINAL ORBITAL PARAMETERS

$a = 12,760$ Km $i = 60°$
$e = .574$ $\omega = 30°$
$\tau = 2.0$ HRS $\Omega = 50°$
     $\mu = 5.5673 \ (10^{11}) \ Km^3/HRS^2$

$\Delta t = .5$ HRS : CURVE 1
$\Delta t = .1$ HRS : CURVE 5
$\Delta t = 1.0$ HRS: CURVE 6
μ NOT ESTIMATED
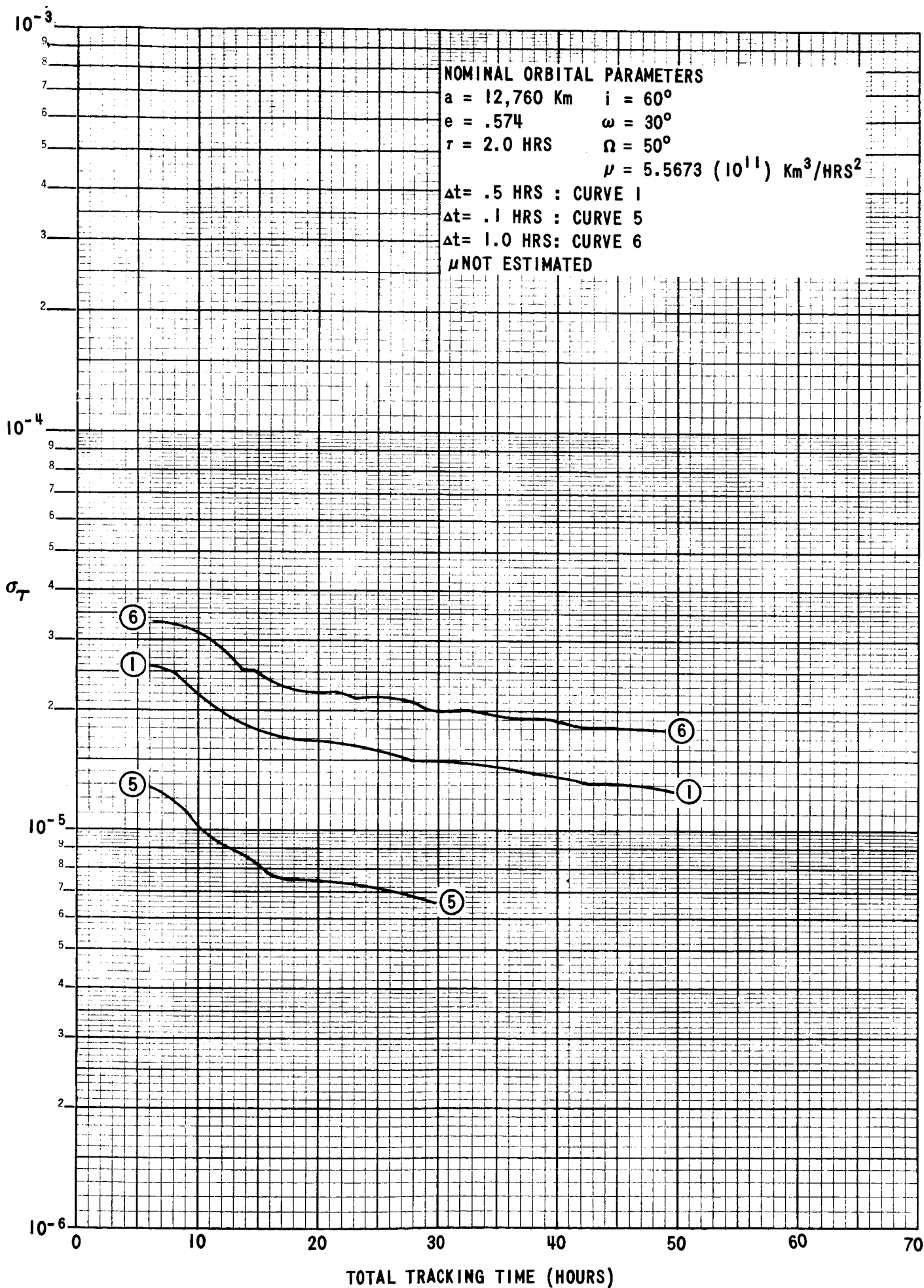
FIGURE 13 – STANDARD DEVIATION OF τ VS TRACKING TIME

NOMINAL ORBITAL PARAMETERS

a = 12,760 Km   i = 60°
e = .574   ω = 30°
τ = 2.0 HRS   Ω = 50°
                 μ = 5.5673 (10^{11}) Km^3/HRS^2
Δt= .5 HRS : CURVE 1
Δt= .1 HRS : CURVE 5
Δt= 1.0 HRS: CURVE 6
μ NOT ESTIMATED

σ_i

TOTAL TRACKING TIME (HOURS)
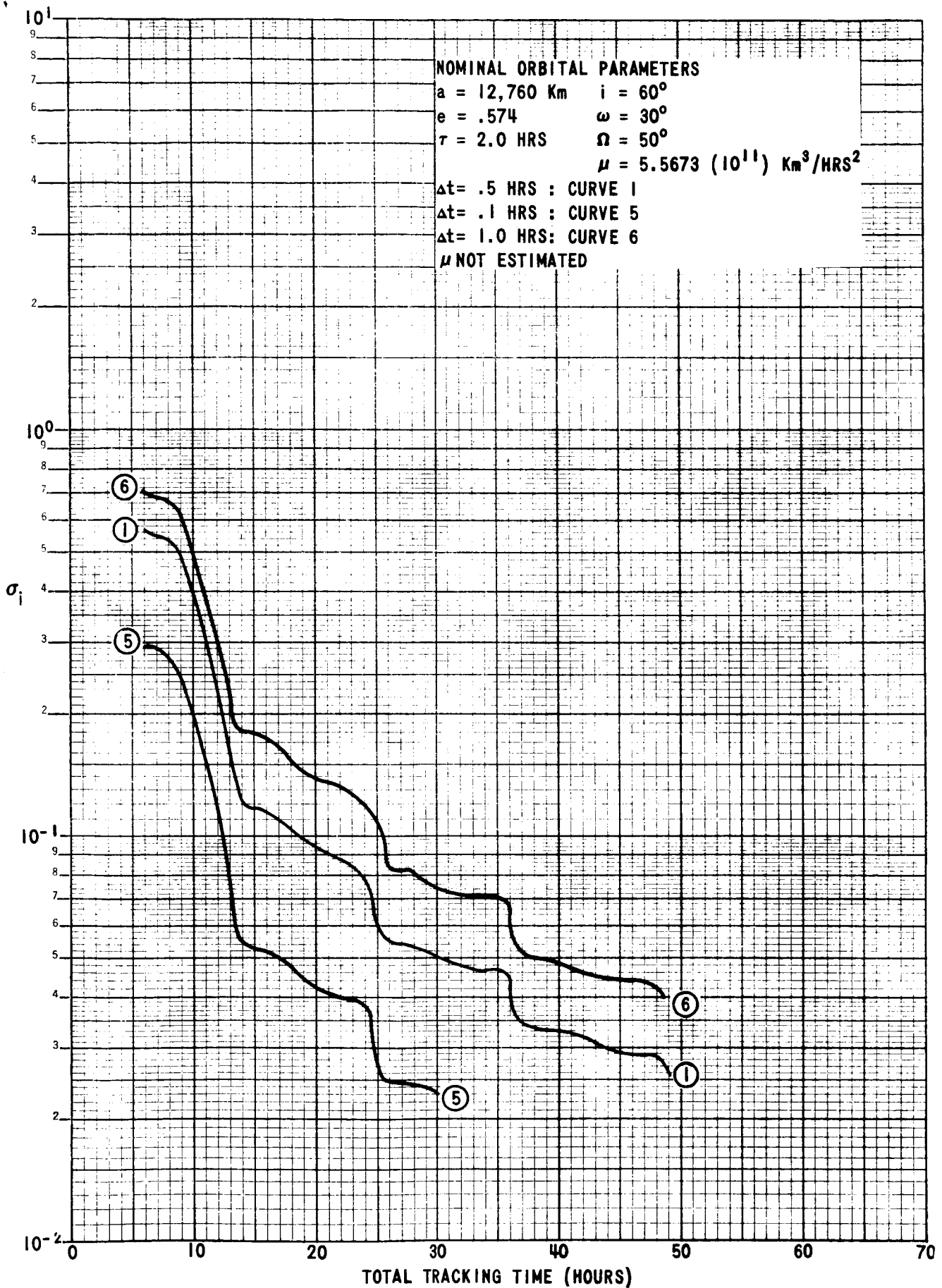
FIGURE 14 - STANDARD DEVIATION OF i VS TRACKING TIME
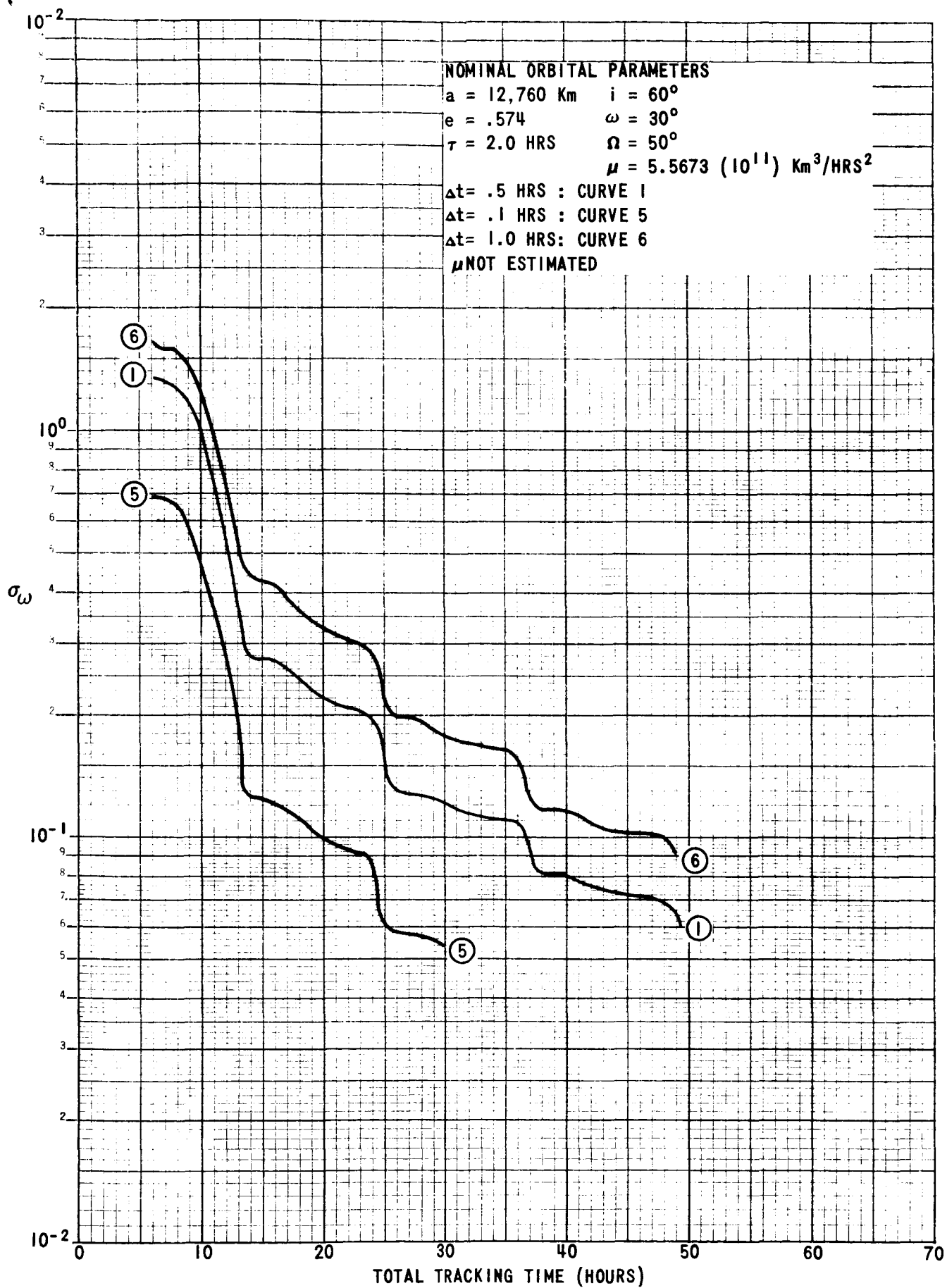
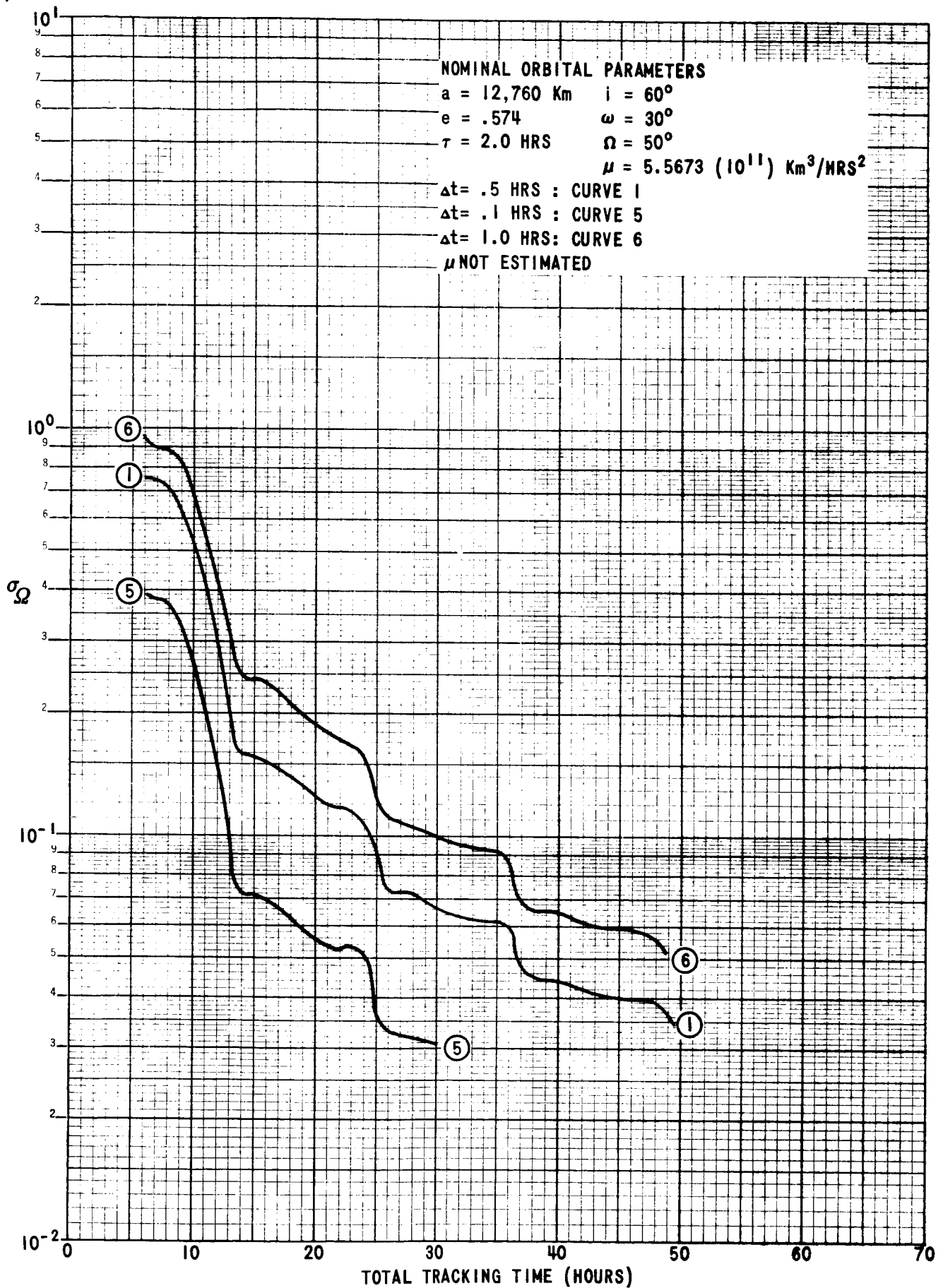FIGURE 15 - STANDARD DEVIATION OF ω VS TRACKING TIME

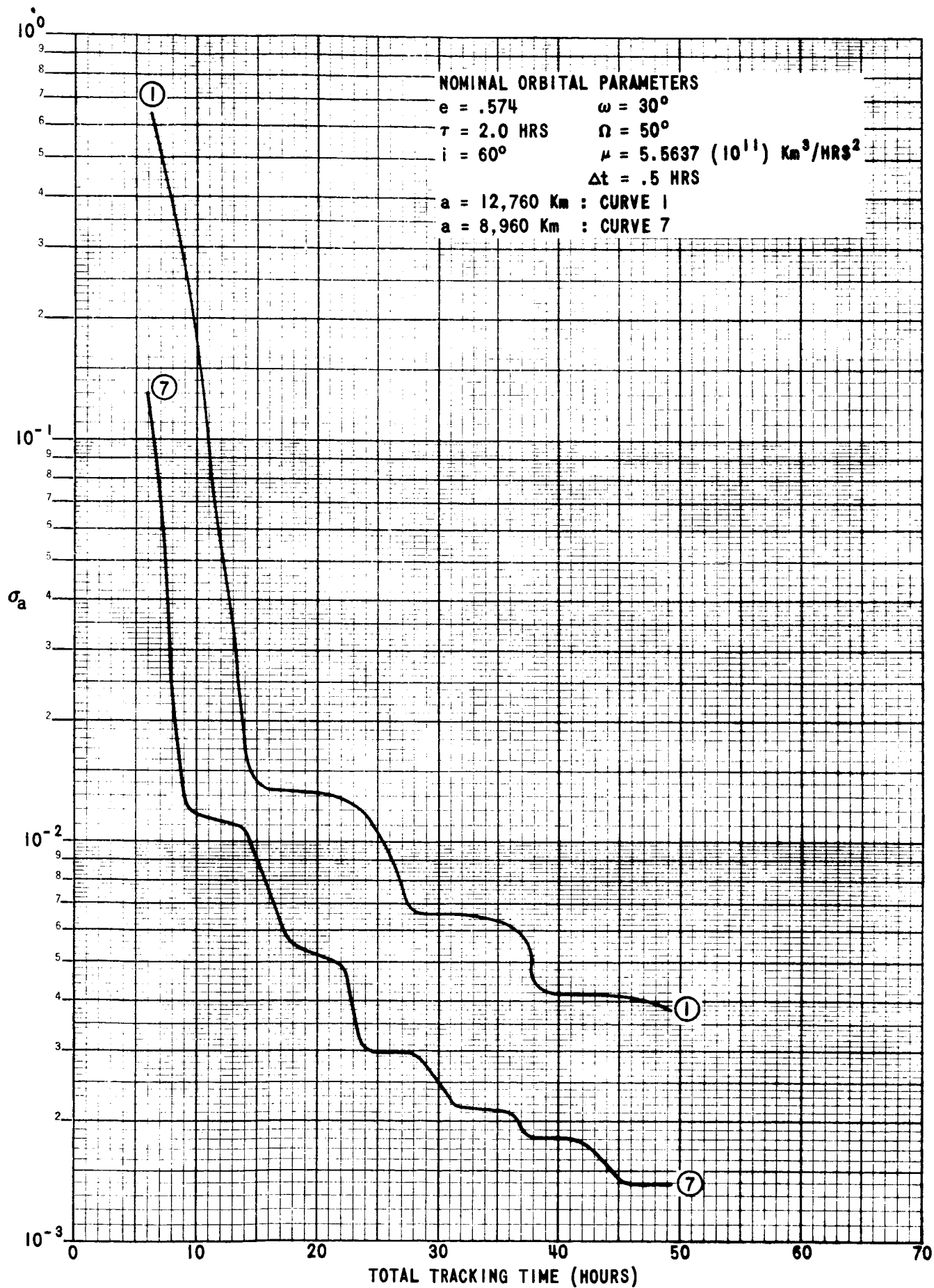NOMINAL ORBITAL PARAMETERS

$a = 12,760$ Km $i = 60°$

$e = .574$ $\omega = 30°$

$\tau = 2.0$ HRS $\Omega = 50°$

$\mu = 5.5673 \ (10^{11}) \ Km^3/HRS^2$

$\Delta t = .5$ HRS : CURVE 1

$\Delta t = .1$ HRS : CURVE 5

$\Delta t = 1.0$ HRS: CURVE 6

μ NOT ESTIMATED

σ_Ω

TOTAL TRACKING TIME (HOURS)

FIGURE 16 — STANDARD DEVIATION OF Ω VS TRACKING TIME

NOMINAL ORBITAL PARAMETERS

$e = .574$ $\omega = 30°$
$\tau = 2.0$ HRS $\Omega = 50°$
$i = 60°$ $\mu = 5.5637 \ (10^{11}) \ Km^3/HRS^2$
$\Delta t = .5$ HRS
$a = 12,760$ Km : CURVE 1
$a = 8,960$ Km : CURVE 7

TOTAL TRACKING TIME (HOURS)

FIGURE 17 – STANDARD DEVIATION OF a VS TRACKING TIME

NOMINAL ORBITAL PARAMETERS
$e = .574$ $\omega = 30°$
$\tau = 2.0$ HRS $\Omega = 50°$
$i = 60°$ $\mu = 5.5637 \ (10^{11}) \ Km^3/HRS^2$
                  $\Delta t = .5$ HRS
$a = 12,760$ Km : CURVE 1
$a = 8,960$ Km : CURVE 7

TOTAL TRACKING TIME (HOURS)
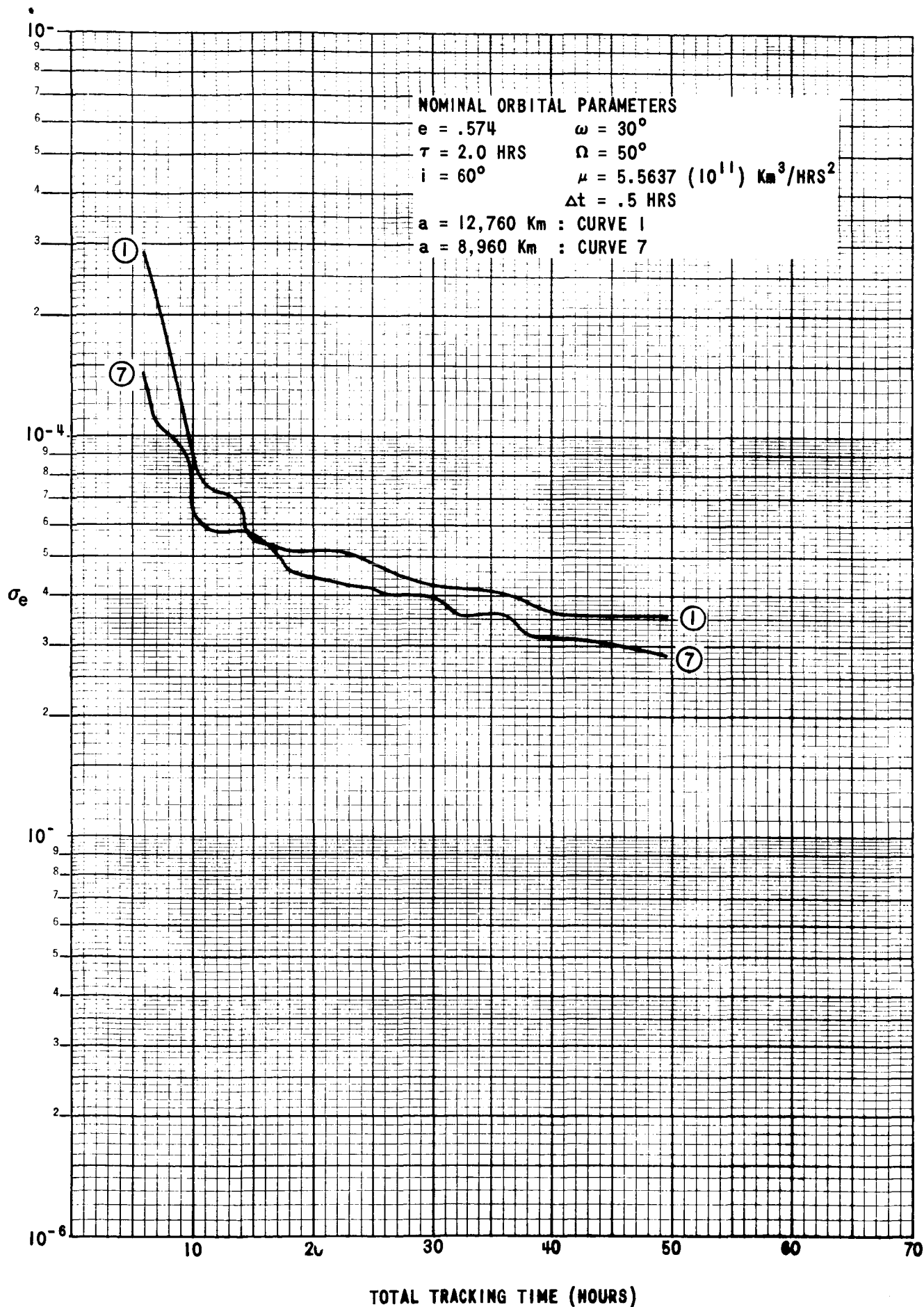
FIGURE 18 - STANDARD DEVIATION OF e VS TRACKING TIME
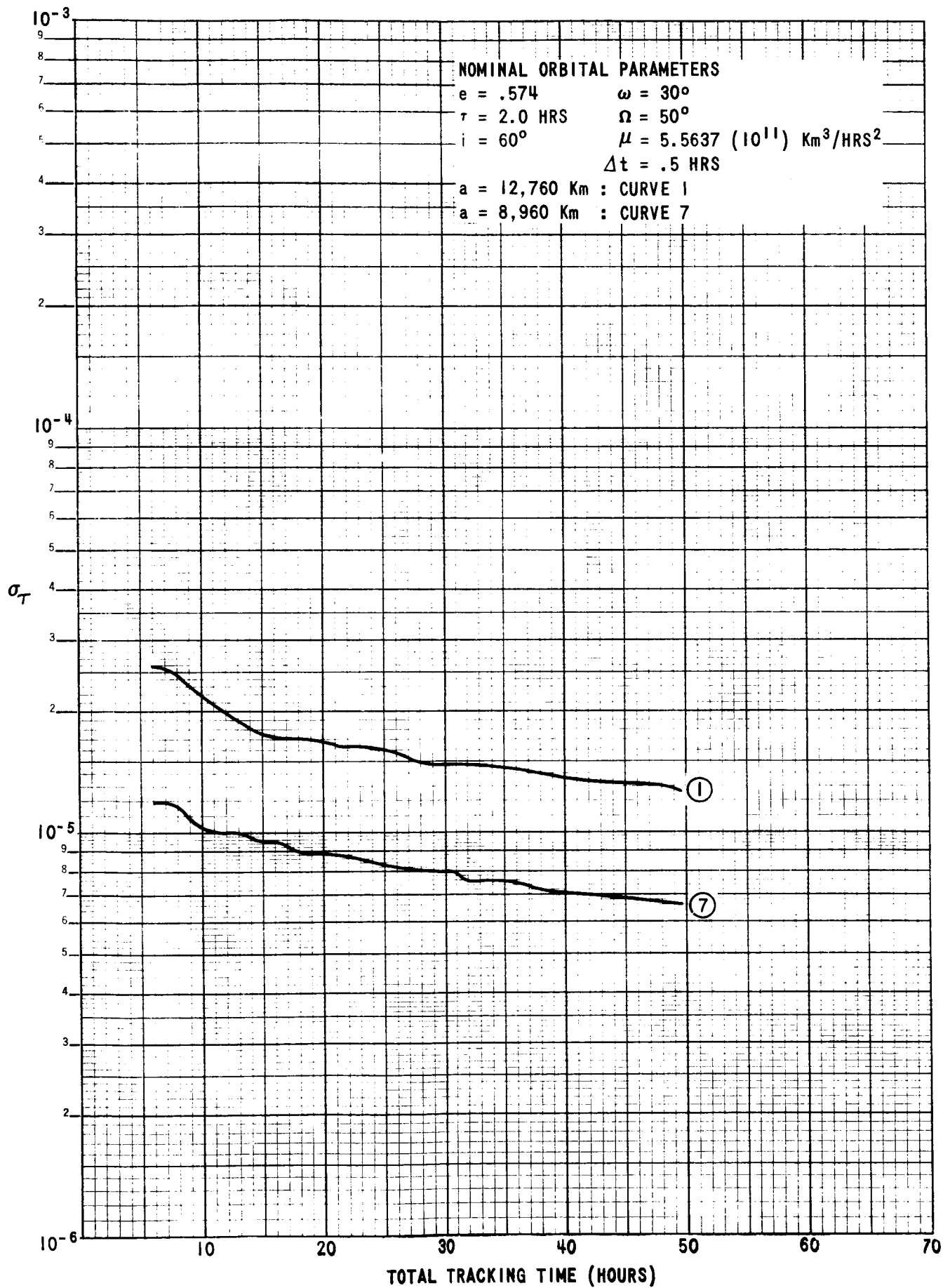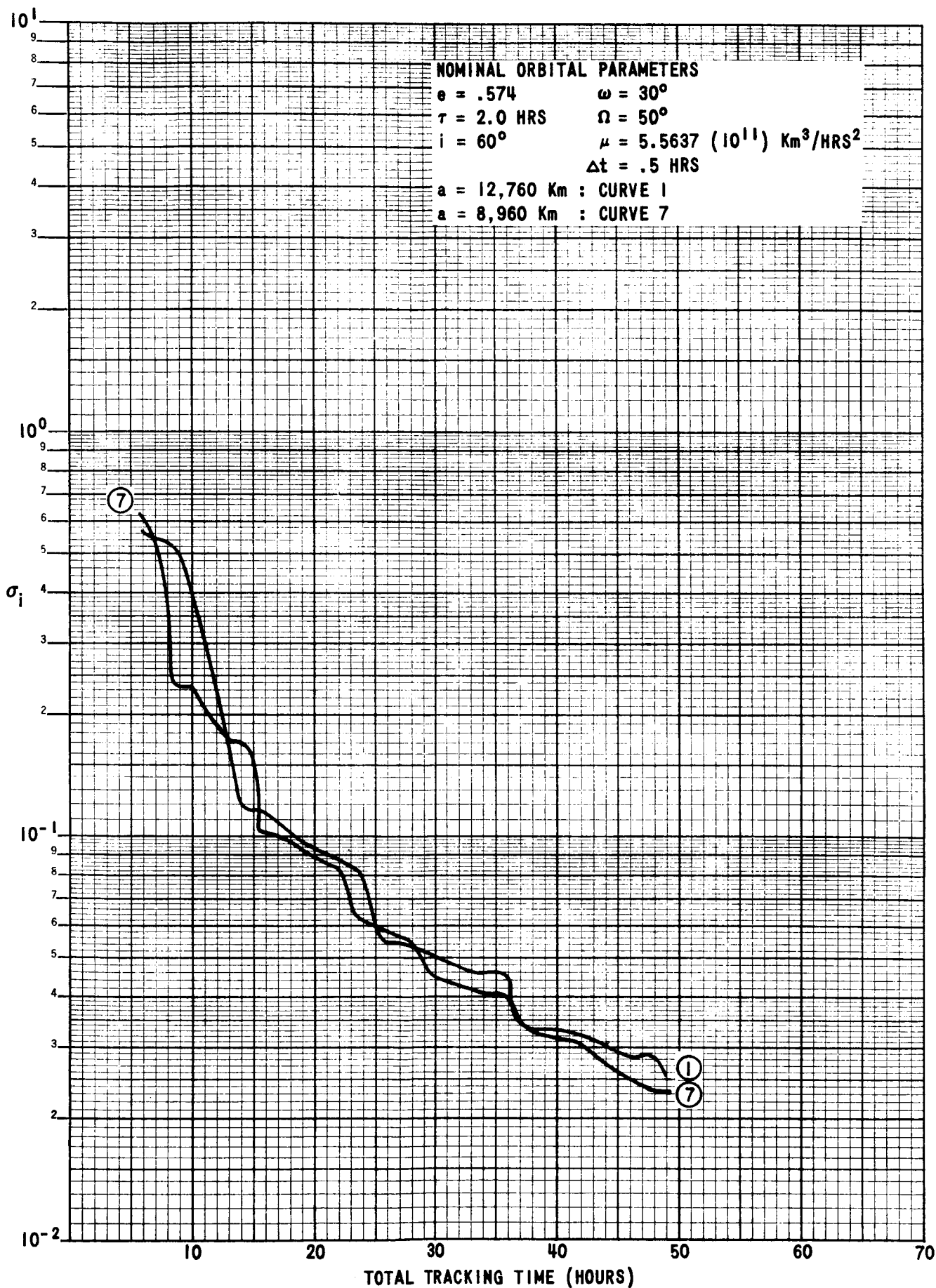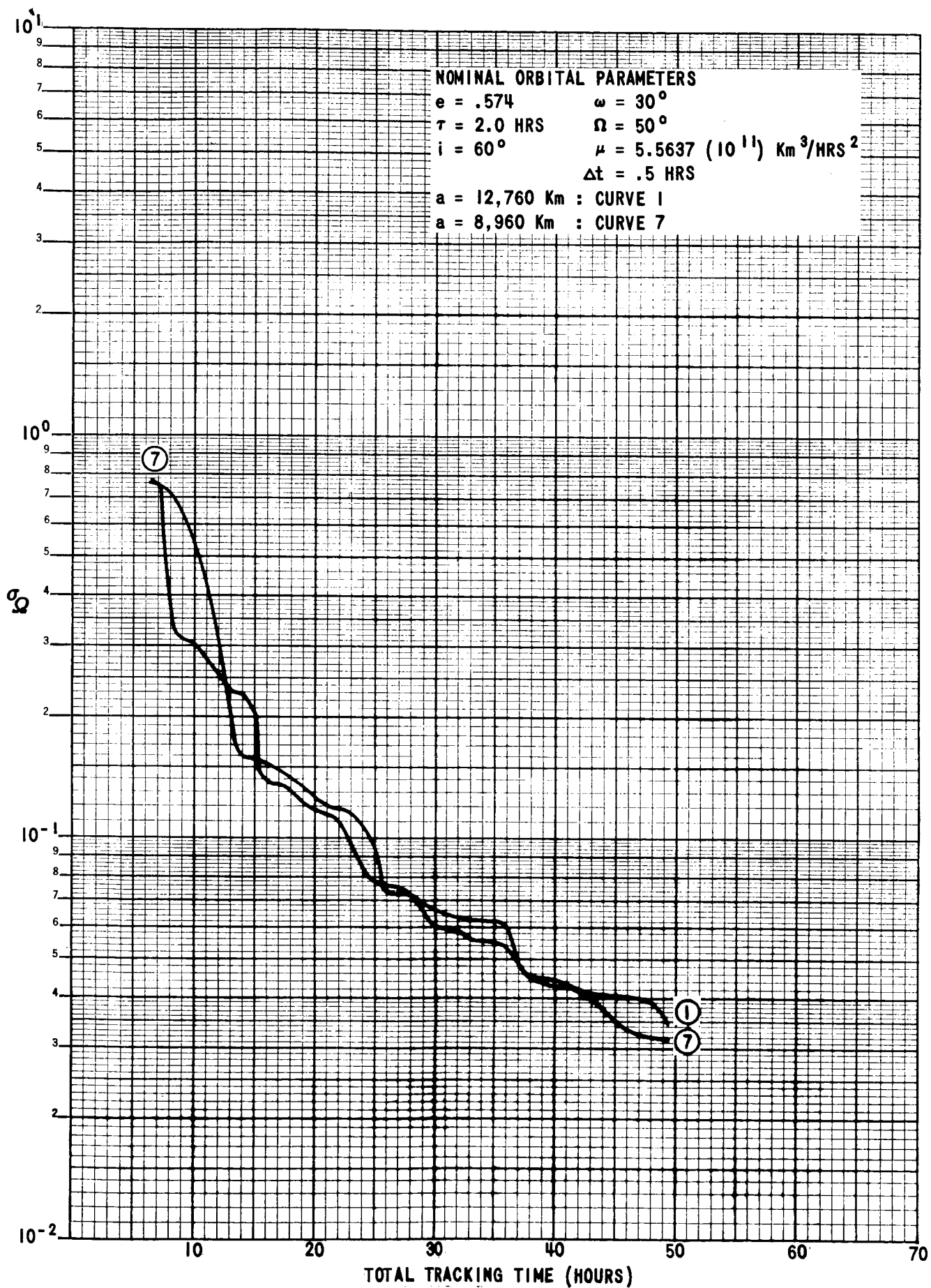
FIGURE 19 - STANDARD DEVIATION OF τ VS TRACKING TIME

NOMINAL ORBITAL PARAMETERS

$e = .574$ $\omega = 30°$
$\tau = 2.0$ HRS $\Omega = 50°$
$i = 60°$ $\mu = 5.5637 \ (10^{11}) \ Km^3/HRS^2$
     $\Delta t = .5$ HRS
$a = 12,760$ Km : CURVE 1
$a = 8,960$ Km : CURVE 7

σ_i

TOTAL TRACKING TIME (HOURS)

FIGURE 20 - STANDARD DEVIATION OF i VS TRACKING TIME
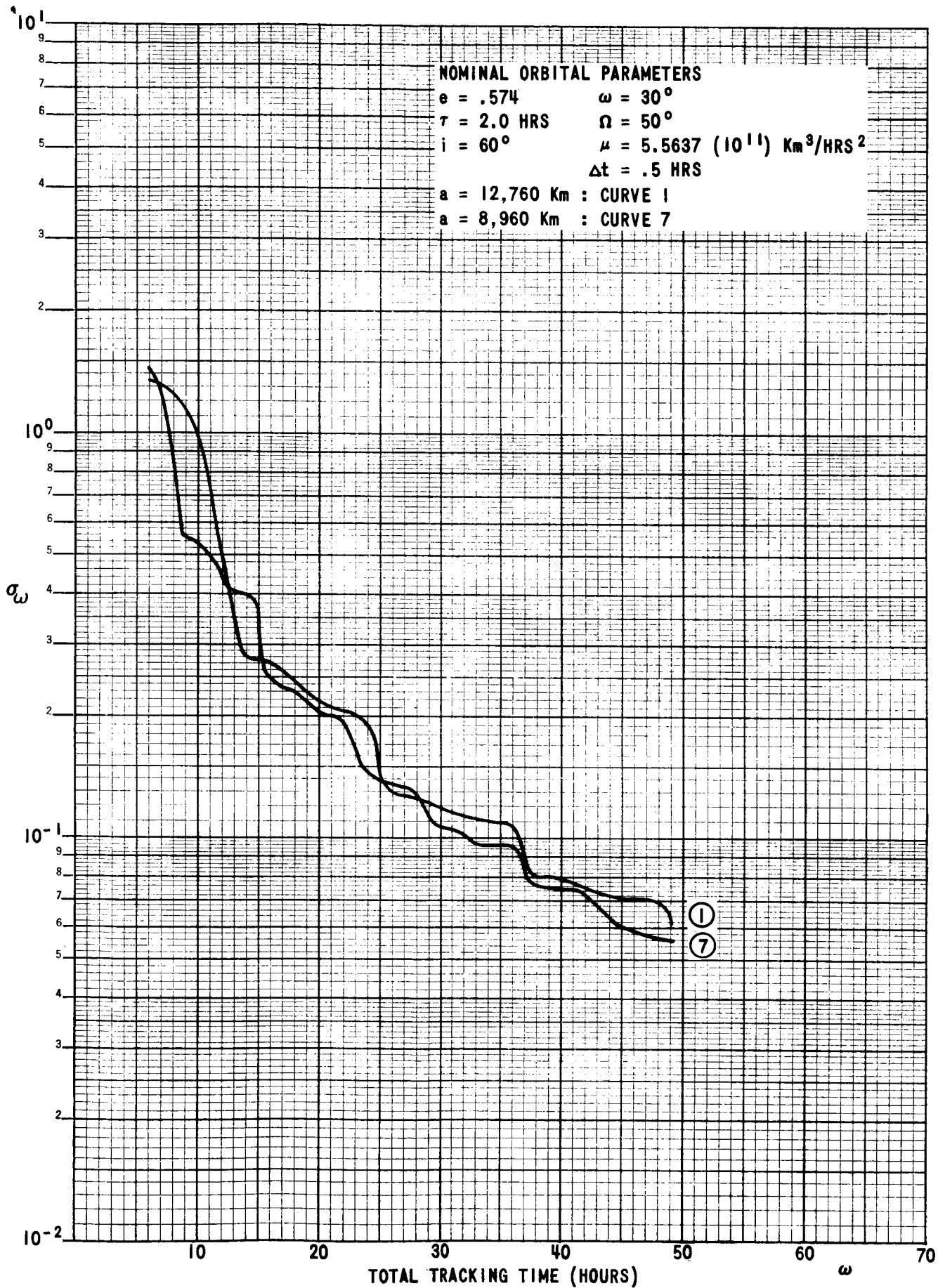
FIGURE 21 - STANDARD DEVIATION OF ω VS TRACKING TIME

NOMINAL ORBITAL PARAMETERS

$e = .574$ $\omega = 30°$
$\tau = 2.0$ HRS $\Omega = 50°$
$i = 60°$ $\mu = 5.5637 \,(10^{11})$ Km^3/HRS^2
$\Delta t = .5$ HRS

$a = 12,760$ Km : CURVE 1
$a = 8,960$ Km : CURVE 7
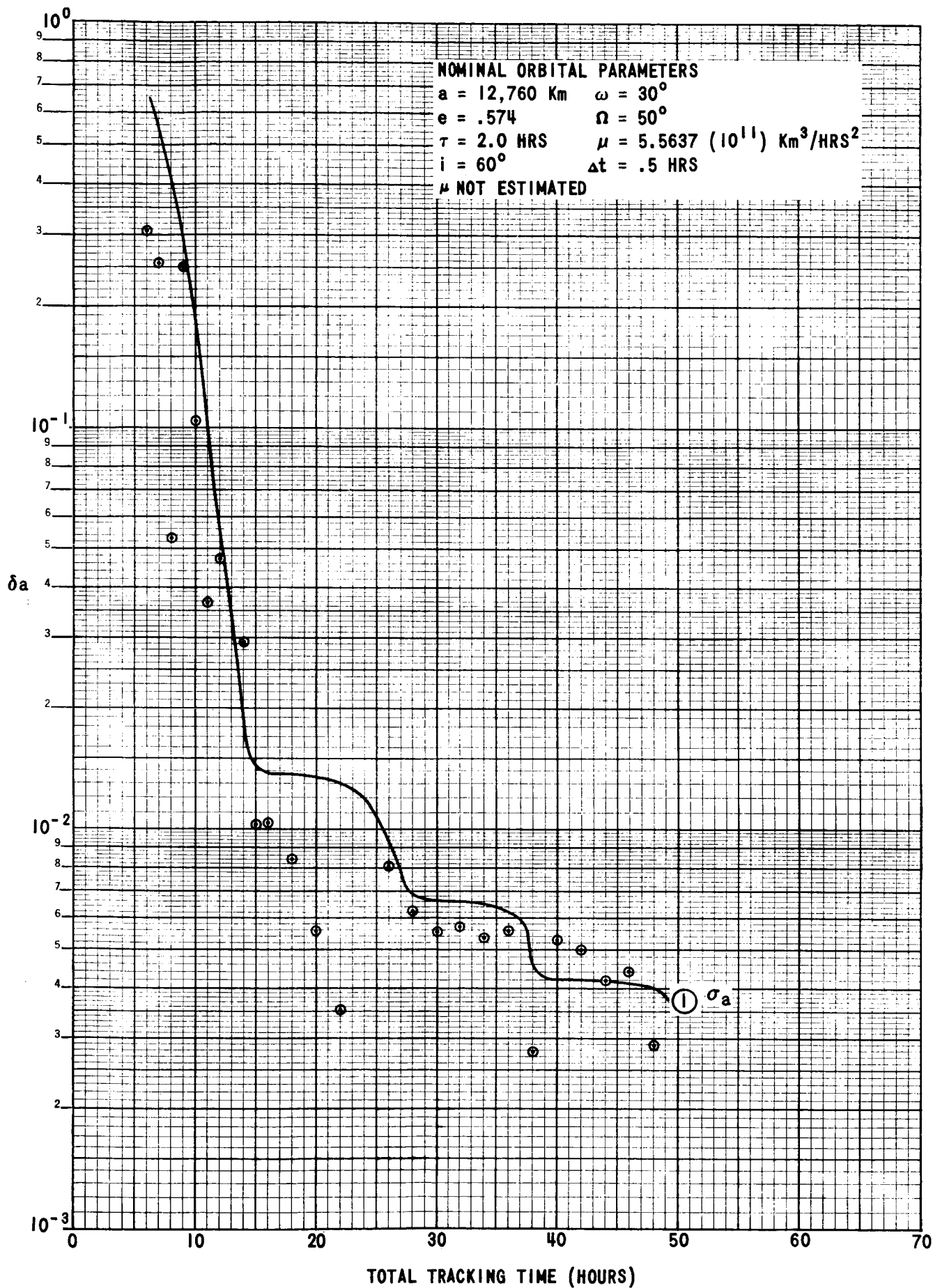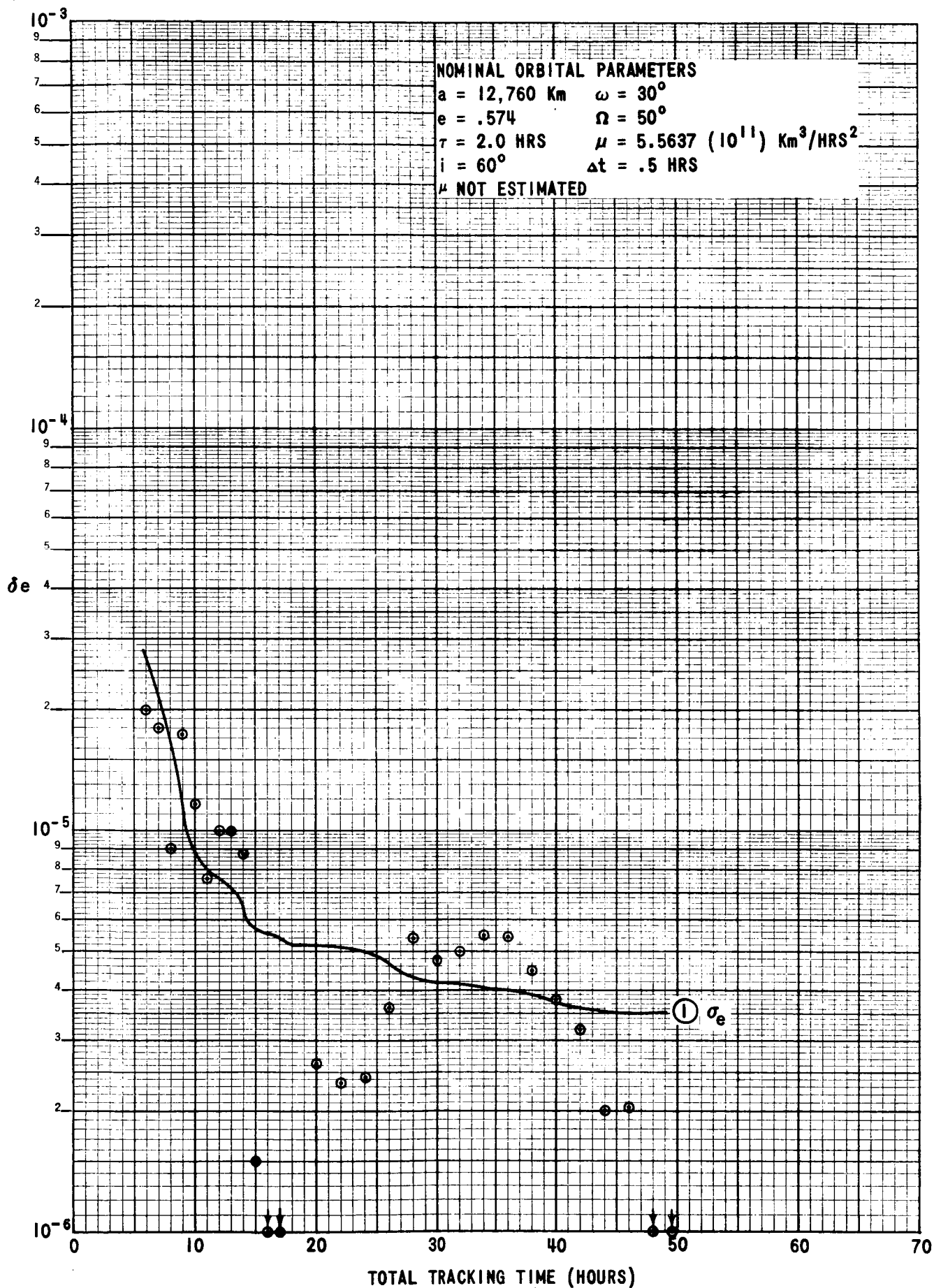
FIGURE 22 - STANDARD DEVIATION OF Ω VS TRACKING TIME

FIGURE 23 - ABSOLUTE ERROR AND STANDARD DEVIATION OF a VS TRACKING TIME

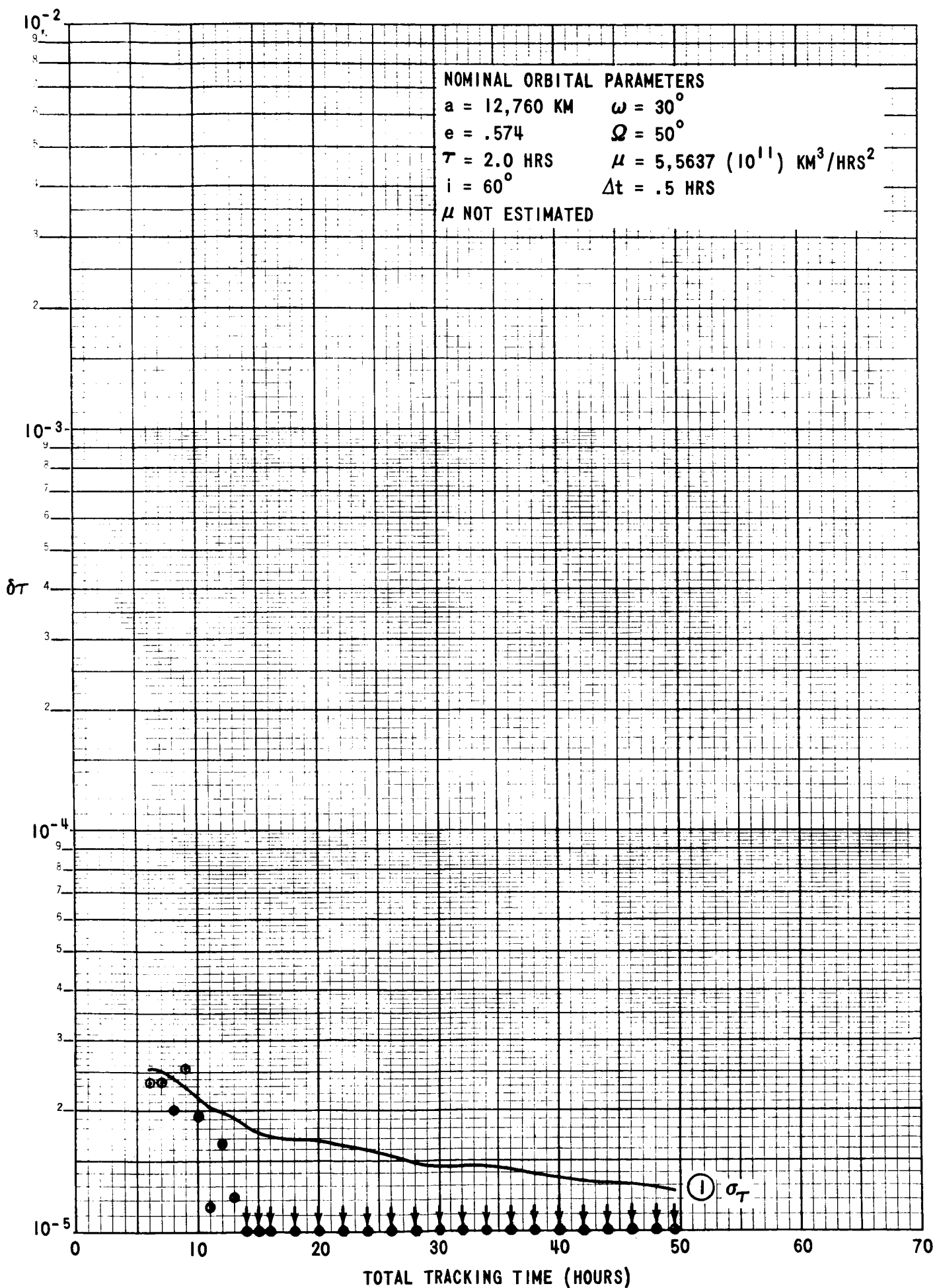FIGURE 24 - ABSOLUTE ERROR AND STANDARD DEVIATION OF e VS TRACKING TIME

NOMINAL ORBITAL PARAMETERS
$a = 12,760$ KM $\omega = 30°$
$e = .574$ $\Omega = 50°$
$\mathcal{T} = 2.0$ HRS $\mu = 5,5637 \, (10^{11})$ KM^3/HRS^2
$i = 60°$ $\Delta t = .5$ HRS
μ NOT ESTIMATED

$\delta \tau$

$\textcircled{1} \, \sigma_\tau$

TOTAL TRACKING TIME (HOURS)

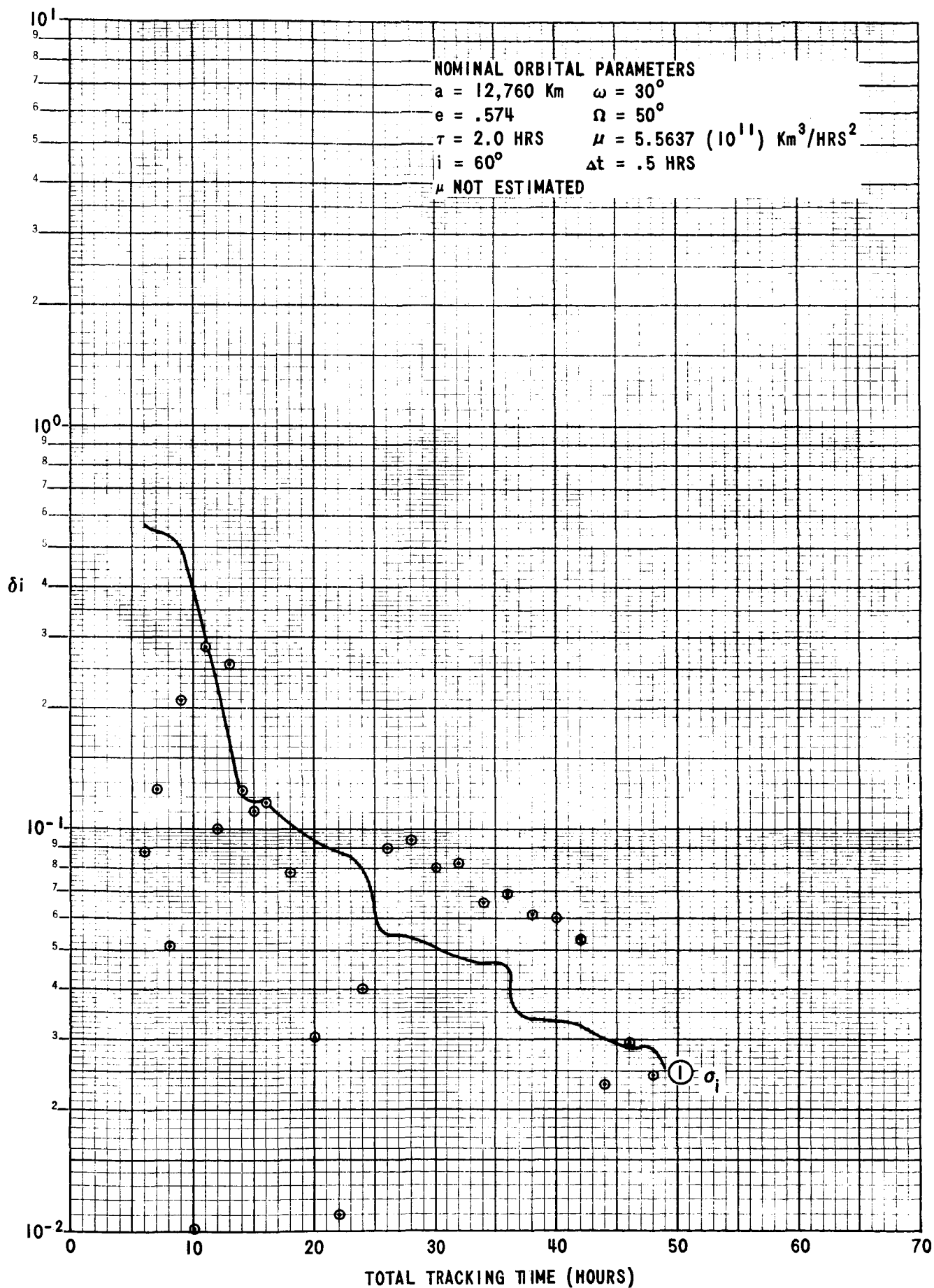FIGURE 25 – ABSOLUTE ERROR AND STANDARD DEVIATION OF τ VS TRACKING TIME

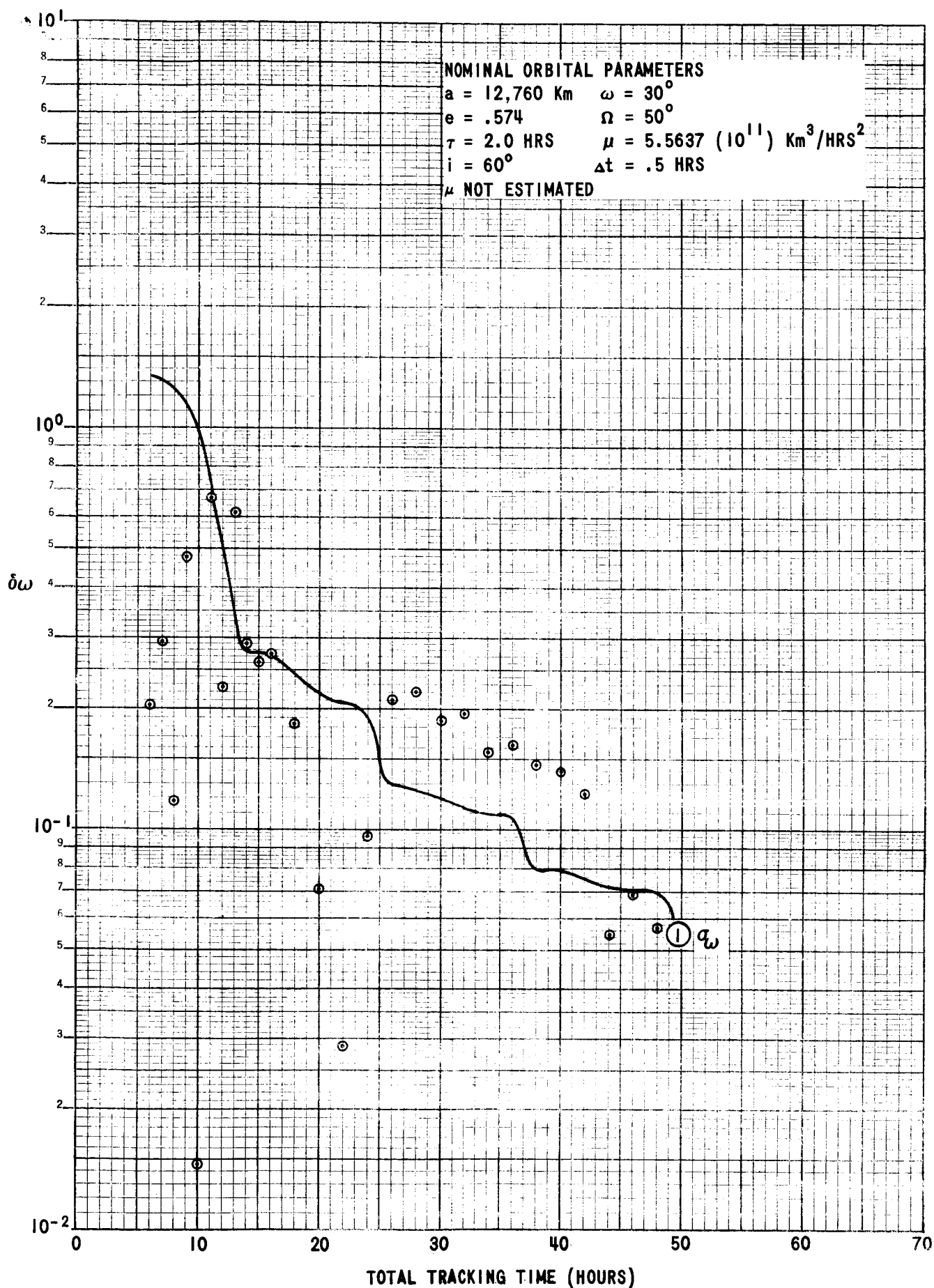FIGURE 26 — ABSOLUTE ERROR AND STANDARD DEVIATION OF i VS TRACKING TIME

FIGURE 27 - ABSOLUTE ERROR AND STANDARD DEVIATION OF ω VS TRACKING TIME

NOMINAL ORBITAL PARAMETERS
a = 12,760 Km ω = 30°
e = .574 Ω = 50°
τ = 2.0 HRS μ = 5.5637 (10^{11}) Km³/HRS²
i = 60° Δt = .5 HRS
μ NOT ESTIMATED

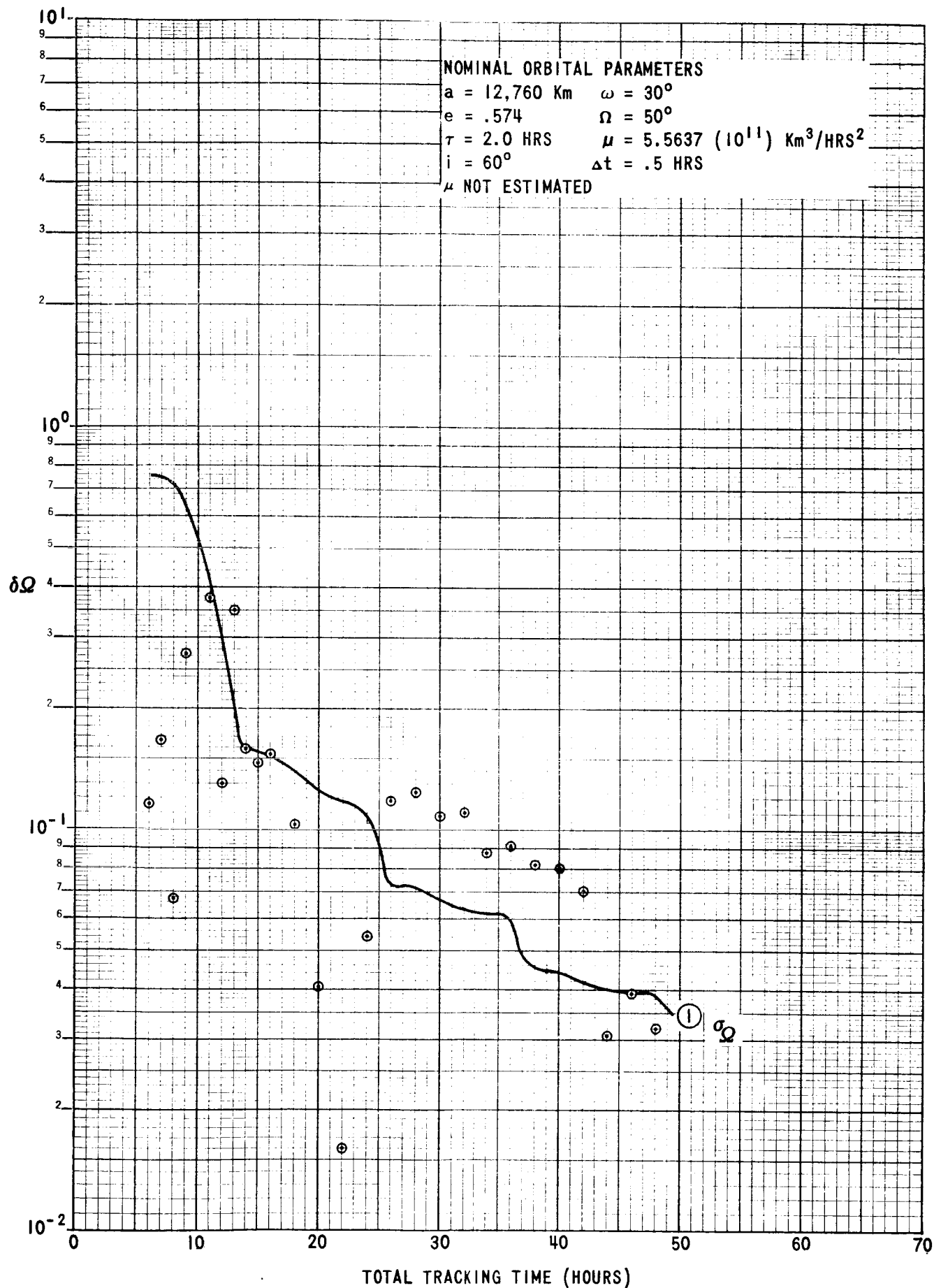σ_{Ω}

TOTAL TRACKING TIME (HOURS)

FIGURE 28 – ABSOLUTE ERROR AND STANDARD DEVIATION OF Ω VS TRACKING TIME